# Theoretical Prediction and Experimental Substantiation of the Response of the Automobile to Steering Control

Leonard Segel

*Proceedings of the Institution of Mechanical Engineers: Automobile Division* 1956 10: 310
DOI: 10.1243/PIME_AUTO_1956_000_032_02

# THEORETICAL PREDICTION AND EXPERIMENTAL SUBSTANTIATION OF THE RESPONSE OF THE AUTOMOBILE TO STEERING CONTROL

By Leonard Segel, M.S., B.S.*

Classical mechanics is applied to the automobile in order to study the lateral rigid-body motions produced by steering control. This research in the field of automotive lateral dynamics has included (1) the development of a mathematical model for a pneumatic-tyred vehicle and (2) its subsequent substantiation by means of full-scale response tests made with an instrumented vehicle. A review of the theoretical work is presented together with a description of the methods used to measure the response of the test car. The resulting agreement between theory and experiment is examined, and is followed by an extensive discussion of the nature of the lateral response of the automobile to steering control.

## INTRODUCTION

THIS PAPER presents a discussion of the theoretical and experimental results obtained during research in the field of automotive lateral dynamics. The two major tasks described herein are the development of a mathematical model to replace the physical automobile and the utilization of full-scale response measurements to check the dynamic behaviour predicted by the derived equations. In accomplishing both tasks, experience acquired by the Flight Research Department, Cornell Aeronautical Laboratory, in studying aircraft dynamic stability and control, proved to be invaluable. Specifically, it was possible to adopt in this research some of the dynamic-recording methods and response-test techniques which had been developed for aircraft work. Also, certain analytical techniques, applicable to problems in aircraft dynamics, were adopted in this particular study of the directional behaviour of the automobile.

In reviewing some of the results achieved to date, the paper will:

(1) describe the development of the lateral equations of motion of the vehicle and their subsequent experimental verification, and

(2) use the derived theory to discuss certain basic steady-state and dynamic properties of the response of the vehicle to steering control.

*The MS. of this paper was received at the Institution on 30th August 1956.*

* *Section Head, Vehicle Dynamics Department, Cornell Aeronautical Laboratory, Inc., Buffalo, New York, United States of America.*

### Notation

| | |
|---|---|
| $A, B, C, E, F$ | Coefficients of stability quartic. |
| $AT$ | Aligning torque produced by two front or rear tyres, ft.-lb. |
| $a$ | Distance between vehicle c.g. and front wheel centre, feet. |
| $b$ | Distance between vehicle c.g. and rear wheel centre, feet. |
| $C$ | $C_1+C_2$, Total cornering stiffness of vehicle, lb. per radian. |
| $C_1$ | $\partial Y/\partial\alpha_1$, Cornering stiffness of both front tyres, lb. per radian. |
| $C_2$ | $\partial Y/\partial\alpha_2$, Cornering stiffness of both rear tyres, lb. per radian. |
| $c$ | Distance between c.g. of rolling mass and the $z$ axis, feet. |
| $D$ | $\tau\frac{d}{dt}$ Non-dimensional derivative operator. |
| $e$ | Distance between c.g. of unsprung (non-rolling) mass and the $z$ axis, feet. |
| $f$ | Frequency, cycles per sec. |
| $g$ | Acceleration of gravity, ft. per sec.$^2$. |
| $h$ | Height of the c.g. of rolling mass above the roll axis, feet. |
| $I_{cg)_s}$ | Moment of inertia of the rolling mass about a horizontal axis through the c.g. of the rolling mass, slug-ft.$^2$. |
| $I_x$ | Moment of inertia of the rolling mass about the $x$ axis, slug-ft.$^2$ |
| $I_{x'}$ | Moment of inertia of the rolling mass about the $x'$ axis, slug-ft.$^2$ |

| | |
|---|---|
| $I_{xz}$ | Product of inertia of the vehicle about the $x$ and $z$ axes, slug-ft.$^2$ |
| $I_{x'z'}$ | Product of inertia of the vehicle about the $x'$ and $z'$ axes, slug-ft.$^2$ |
| $I_z$ | Moment of inertia of the vehicle about the $z$ axis, slug-ft.$^2$ |
| $j$ | $\sqrt{-1}$. |
| $k$ | Roll stiffness of suspension, ft.-lb. per radian. |
| $k_z$ | Radius of gyration of vehicle mass about the $z$ axis, feet. |
| $L$ | Rolling moment about $x$ axis, ft.-lb. |
| $l$ | Wheelbase, feet. |
| $M$ | Total mass of vehicle, slugs. |
| $M_s$ | Rolling mass of vehicle, slugs. |
| $M_u$ | Non-rolling (unsprung) mass of vehicle, slugs. |
| $N$ | Yawing moment about $z$ axis, ft.-lb. |
| $n_y$ | Total lateral acceleration along the $y$ axis, $g$ units. |
| $p$ | Rolling velocity around $x$ axis, radians per sec. |
| $R$ | Radius of steady-state turn, feet. |
| $r$ | Yawing velocity around $z$ axis, radians per sec. |
| $\hat{r}$ | $r\tau$, Non-dimensional yawing velocity, radians. |
| S.M. | Static margin (non-dimensional). |
| $s$ | Laplacian operator or argument. |
| $t$ | Tread of vehicle, feet. |
| $V$ | Forward velocity of vehicle, ft. per sec. |
| $v$ | Lateral velocity of vehicle along $y$ axis, ft. per sec. |
| $W_s$ | Weight of rolling mass, lb. |
| $X$ | Rolling resistance of tyre, lb. |
| $x, y, z$ | Body axes fixed in vehicle with origin on the roll axis. |
| $x', y', z'$ | Body axes fixed in vehicle with origin at the centre of gravity (c.g.). |
| $x_u, y_u, z_u$ | Body axes fixed in vehicle with origin at the c.g. of the non-rolling mass. |
| $Y$ | Force along $y$ axis, lb. |
| $\bar{y}$ | Lateral displacement of the c.g. of the rolling mass, feet. |
| $Z$ | Vertical load on tyre, lb. |
| $z$ | Height of roll axis above ground. |
| $\alpha$ | Tyre slip angle, radians. |
| $\beta$ | Side-slip angle of vehicle, radians. |
| $\gamma$ | Camber angle of front wheels, radians. |
| $\Delta Z$ | Vertical load transfer, lb. |
| $\delta$ | Steer angle of front wheels, radians. |
| $\partial AT/\partial\alpha$ | Slip of aligning torque *versus* wheel slip angle, ft.-lb. per radian. |
| $\partial L/\partial p$ | Roll damping produced by the shock absorbers, ft.-lb.-sec. per radian. |
| $\partial X/\partial Z$ | Change in rolling resistance with change in tyre vertical loading, lb. per lb. |
| $\partial Y_1/\partial\gamma$ | Camber thrust per unit camber angle of front wheels, lb. per radian. |
| $\partial\gamma/\partial\phi$ | Rate of change of front wheel camber with respect to body roll, radians per radian. |
| $\epsilon_2$ | $\partial\delta_2/\partial\phi$, Rear roll steer, radians per radian. |
| $\lambda_1, \lambda_2$ | Roots of the characteristic equation, 1/sec. |
| $\mu$ | $V/\sqrt{(lg)}$, Vehicle Froude number. |
| $\tau$ | $\sqrt{(l/g)}$, sec. |
| $\phi$ | Roll angle of the vehicle, radians. |
| $\varphi$ | Phase angle, deg. |
| $\varphi_{a_b}$ | Phase angle of $a$ with respect to $b$, deg. |
| $\omega$ | Circular frequency, radians per sec. |
| $\lvert\ \rvert$ | Absolute value or amplitude. |

Subscripts:

| | |
|---|---|
| $ss$ | Steady state. |
| 1 | Front-wheel position. |
| 2 | Rear-wheel position. |

Note: A dot over a symbol means time rate of change.

## A LINEAR MATHEMATICAL MODEL OF THE AUTOMOBILE

### Philosophy of Approach

Milliken has pointed out that, in the process of creating a mathematical model for the automobile, it is desirable to treat the automobile as a linear dynamic system. There are many advantages to be gained by doing so. In particular, the application of many of the experimental techniques developed for studying dynamic systems requires the existence of linearity. Linear behaviour was accordingly the first assumption made in developing a mathematical model of the automobile. It will be seen later that this assumption is quite adequate for lateral motions of a reasonable magnitude.

Since the principle of superposition applies for linear dynamic systems, this first assumption makes it possible to break down the complicated overall problem of vehicle stability and control into its simpler parts. First it was recognized that there are three different types of input to the car, namely: steering, road, and aerodynamic inputs. In the initial attack on the problem, study was made of the vehicle response to steering inputs and study of the response to the latter two inputs was temporarily set aside. Further simplifications were made by differentiating between steering-wheel displacement and steering-torque inputs. Although the human driver steers his car by a combination of wheel displacement and feel, it is possible to study the responses to these two types of steering input separately. The stability and control characteristics associated with a fixed steering wheel or the response produced by a steering-wheel displacement have been called the 'fixed-control' characteristics, in accordance with established aeronautical practice. Conversely, the characteristics associated with a free steering wheel or the response produced by a steering torque have been designated the 'free-control' behaviour or response.

This distinction is shown schematically in Fig. 4 in which a torque or displacement is shown imposed on the steering wheel, producing an angular displacement of the front wheels. The front wheels in turn impose a side force and turning moment on the car, and directional manoeuvring of the vehicle results.

The complete dynamic system pictured in Fig. 4 may be simplified even further by neglecting the steering system

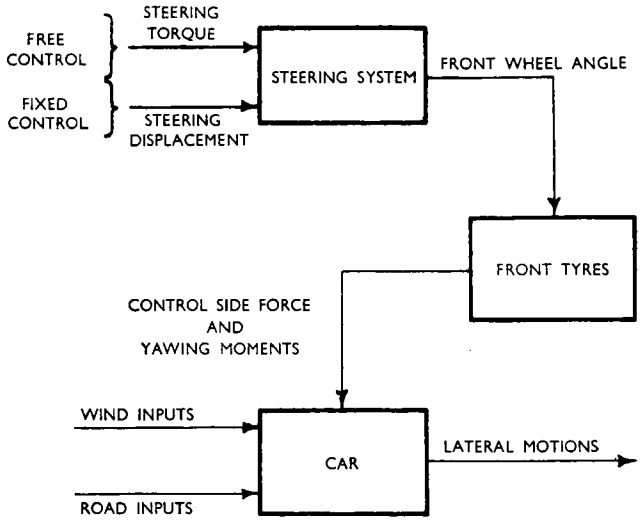


*Fig. 4. Representation of Fixed and Free Control*

and considering the vehicle response to front-wheel angle displacement. Note that the essential car dynamics are contained in the 'black box' at the bottom of this figure, and that side force and yawing moments produced by road and wind inputs act on this same 'black box'. Thus, efforts were first directed to develop a mathematical model for that part of the overall vehicle dynamic system represented by the 'black box' labelled 'CAR'.

## Additional Simplifications

Initial studies were therefore restricted to the fixed-control automobile in which the front-wheel steering angle was considered to produce the only force and moment input. With forward velocity considered to be constant during any lateral manoeuvre, the assumption was made that the ride motions of the car (Fig. 5) do not exert any influence on the lateral motions and that the pitching and bouncing degrees of freedom may therefore be neglected when a mathematical model is formulated to describe directional behaviour of the vehicle. Such a model includes forward velocity as one of the major stability parameters, but does not consider forward velocity to be a variable of motion. Furthermore, it was assumed that, during a constant-velocity manoeuvre, driving thrust (1) remains fixed, (2) is split equally between the two rear wheels, and (3) does not affect the lateral mechanical properties of the rear tyres for the range of velocities treated in this study.

Simplifications were also made in representing the mass

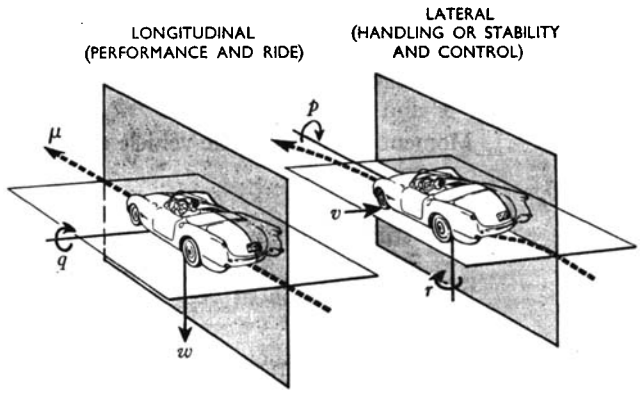


*Fig. 5. Car Motions*

of an automobile. In this study, the automobile was considered to be a two-mass system consisting of a rolling mass and non-rolling mass, with the rolling mass constrained to roll about an axis fixed in the non-rolling mass. This axis is, of course, the 'roll axis', which is located by the kinematic properties of the front and rear suspensions.

## The d'Alembert or Inertia Forces

To write the equations of motion of the automobile, the time rate of change of momentum and of moment of momentum must be measured with respect to inertial space. If the motion of the automobile is given relative to space axes, the problem becomes unwieldy, for the moment of inertia tensor will vary from instant to instant. To overcome this difficulty, a moving axis system is fixed in the automobile. Fig. 6 shows in detail the body axes that were adopted for the automobile and the nomenclature used to describe the lateral motions of the car. In this treatment, the roll axis was replaced by the $x$ stability axis which is parallel to the ground and is located vertically by the intersection

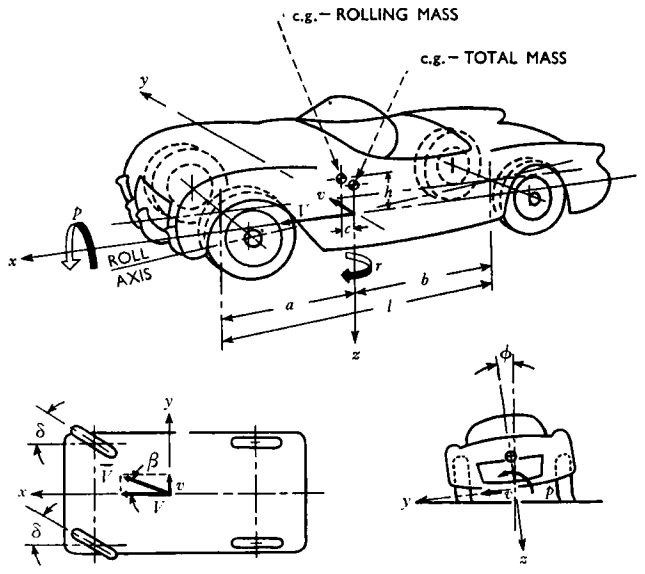


*Fig. 6. Axis System for Simplified Automobile*

of the vertical $z$ axis (passing through the centre of gravity of the entire car) and the actual roll axis of the vehicle. It should be noted that the $z$ axis lies in the plane of symmetry of the rolling mass and that the $y$ axis is perpendicular to the plane of symmetry. The lateral velocity, $v$, and the yawing velocity, $r$, are defined with respect to this axis system which tilts with respect to the ground plane. For small roll angles, however, the lateral velocity, $v$, along the inclined $y$ axis will be equivalent to a lateral velocity in the ground plane. Similarly, the yawing velocity, $r$, around the tilted $z$ axis will be equivalent to a yawing velocity about an axis perpendicular to the ground plane. (A later treatment employed an axis system fixed in the unsprung or non-rolling mass, and yielded results identical with those obtained with body axes fixed in the rolling mass.) On the plan view (Fig. 6) it is seen that the sideslip angle, $\beta$, may be alternatively used to describe the motion along the $y$ axis or lateral motion in the equivalent ground plane. For small angles of sideslip, it is assumed that the velocity along the $x$ axis, $V$, is equal to the resultant total velocity of the vehicle.

To derive the inertia reaction terms, the assumption was made that the principal axes of the rolling mass are parallel to the assumed body axes and that the centre of gravity of the non-rolling mass is located on the $x$ axis as shown in Fig. 7. If the space rate of change of linear and angular momenta is expressed with respect to an axis system having its origin at the c.g. of the entire car, there is obtained, following a procedure such as is outlined by Perkins and Hage [153]:

$$\Sigma Y' = M(\dot{v}'+Vr) \quad . \quad . \quad . \quad . \quad . \quad (1)$$

$$\Sigma N' = I_{z'}\dot{r}+I_{x'z'}\dot{p} \quad . \quad . \quad . \quad . \quad . \quad (2)$$

$$\Sigma L' = I_{x'}\dot{p}+I_{x'z'}\dot{r} \quad . \quad . \quad . \quad . \quad . \quad (3)$$

where

$$I_{x'z'} = \frac{M_s M_u}{M} h(c+e) = M_s hc$$

Equations (1) through (3) may be transformed to the $x$, $y$, $z$, axes by noting that

$$\dot{v}' = \dot{v}+\frac{M_s}{M}h\dot{p} \quad . \quad . \quad . \quad . \quad (4)$$

and

$$\Sigma L = \Sigma L'+\frac{M_s}{M}h\Sigma Y' \quad . \quad . \quad . \quad (5)$$

The d'Alembert forces and moments with respect to the desired axis system are finally obtained as

$$\Sigma Y = M(\dot{v}+Vr)+M_s h\dot{p} \quad . \quad . \quad . \quad (6)$$

$$\Sigma N = I_z\dot{r}+I_{xz}\dot{p} \quad . \quad . \quad . \quad . \quad . \quad . \quad (7)$$

$$\Sigma L = I_x\dot{p}+M_s h(\dot{v}+Vr)+I_{xz}\dot{r} \quad . \quad . \quad (8)$$

where

$$I_z = I_{z'}$$

$$I_{xz} = I_{x'z'}$$

$$I = I_{x'}+M\left(\frac{M_s}{M}h\right)^2 = I_{cg})_s+M_s h^2$$

In equation (6), it is seen that the side-force inertia reaction terms, from left to right, are respectively the result of (1) linear and (2) centrifugal acceleration of the total mass, and (3) linear acceleration of the c.g. of the rolling mass caused by rolling acceleration about the roll axis. Equation (7) indicates that the external yawing moment is equal to the product of yawing moment of inertia and yawing acceleration plus the product of rolling acceleration and the product of inertia, $I_{xz}$. The d'Alembert moment about the roll axis, as given in equation (8), is equal to the product of the rolling moment of inertia and rolling acceleration plus the moment of the linear and centrifugal acceleration of the rolling mass about the roll axis plus the product of yawing acceleration and the product of inertia.

## The External Forces and Moments Acting on an Automobile

The desired mathematical model is obtained on equating the inertia reactions (side force, yawing moment, and rolling moment) to their respective external force and moment summations. The external side force and yawing moment acting on the automobile are created in the ground plane and are derived from the force reactions between the tyre and the road. The roll moment about the roll axis, on the other hand, is produced by the spring suspension, the shock absorbers, and gravitational forces.

As indicated earlier, the external forces and moments are assumed to be linear functions of the independent variables of motion. This assumption appears to be valid, since tyre data acquired to date (see References) indicate that the side-force and moment properties of a pneumatic tyre do vary linearly with the slip and camber angles, if these angles are restricted to reasonably small amplitudes. As defined in the literature, slip angle is the angle between the centre plane of the tyre and its direction of motion, and camber angle is the tilt of the tyre centre plane with respect to the vertical.

In the nomenclature developed in both the tyre and automotive industries, the side force produced by a tyre operating at a slip angle is called the 'cornering force', and the moment about a vertical axis through the tyre centre is called the 'aligning torque'. Similarly, side force produced

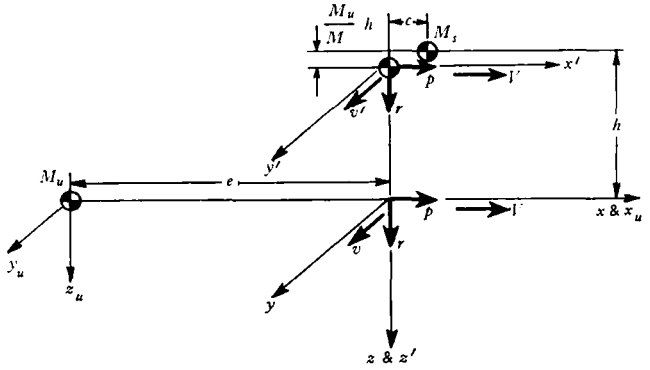


*Fig. 7. Axis Systems Used to Derive Inertia Reactions*

by a cambered tyre has been termed 'camber thrust'. The slope of the cornering-force curve *versus* slip angle is $\partial Y/\partial\alpha$, and this property has been called the 'cornering stiffness', $C$. No similar terminology exists for the slopes of the aligning torque and camber thrust curves and these properties are respectively designated $\partial AT/\partial\alpha$ and $\partial Y/\partial\gamma$. Although existing tyre data show that $C$, $\partial AT/\partial\alpha$, and $\partial Y/\partial\gamma$ are influenced by change in vertical loading of the tyre, the variation in these properties with normal load is neglected in order to retain linearity. Experience has shown, however, that this effect is one of second order, since the combined properties of both front and of both rear tyres are approximately constant for lateral accelerations up to $0{\cdot}3g$.

If load transfer is neglected, the automobile can be considered to be collapsed into the $x$–$z$ plane and to possess one front and rear wheel exhibiting the total properties of both the left and right wheels. When considering the yawing moments produced by unsymmetrical changes in rolling resistance, as are caused by load transfer between the right and left wheels, the wheel tread is, of course, significant. This variation in rolling resistance with vertical loading of the tyre is denoted by the derivative, $\partial X/\partial Z$.

The forces and moments acting on this simplified automobile are shown in Fig. 8. The subscript 1 denotes forces and moments arising from the front tyres and the subscript 2 is used for the rear tyres.

From Fig. 8*a*:

$$\Sigma Y = Y_1+Y_2 \quad . \quad . \quad . \quad . \quad (9)$$

From Fig. 8*a* and *b*:

$$\Sigma N = aY_1+AT)_1+t_1X_1-bY_2+AT)_2+t_2X_2 \quad . \quad (10)$$

From Fig. 8*c*:

$$\Sigma L = W_s\bar{y}+L)_{\text{springs}}+L)_{\text{shock absorbers}} \quad . \quad (11)$$

Note that the right-hand sides of equations (9), (10), and (11) can be expressed in terms of the assumed linear tyre and suspension characteristics of the automobile. From the previous discussion, it is seen that:

$$Y_1 = C_1\alpha_1+\frac{\partial Y_1}{\partial\gamma}\frac{\partial\gamma}{\partial\phi}\phi \quad . \quad . \quad (12)$$

$$Y_2 = C_2\alpha_2 \quad . \quad . \quad . \quad . \quad . \quad (13)$$

$$AT)_1 = \frac{\partial AT}{\partial\alpha_1}\alpha_1 \quad . \quad . \quad . \quad . \quad . \quad (14)$$

$$AT)_2 = \frac{\partial AT}{\partial\alpha_2}\alpha_2 \quad . \quad . \quad . \quad . \quad . \quad (15)$$

$$X_1 = \frac{\partial X}{\partial Z}\Delta Z_1 \quad . \quad . \quad . \quad . \quad . \quad (16)$$

$$X_2 = \frac{\partial X}{\partial Z}\Delta Z_2 \quad . \quad . \quad . \quad . \quad . \quad (17)$$

$$\bar{y} = h\phi \quad . \quad . \quad . \quad . \quad . \quad . \quad (18)$$

$$L)_{\text{springs}} = (k_1+k_2)\phi = k\phi \quad . \quad . \quad (19)$$

$$L)_{\text{shock absorbers}} = \left[\left(\frac{\partial L}{\partial p}\right)_1+\left(\frac{\partial L}{\partial p}\right)_2\right]p \quad . \quad . \quad (20)$$

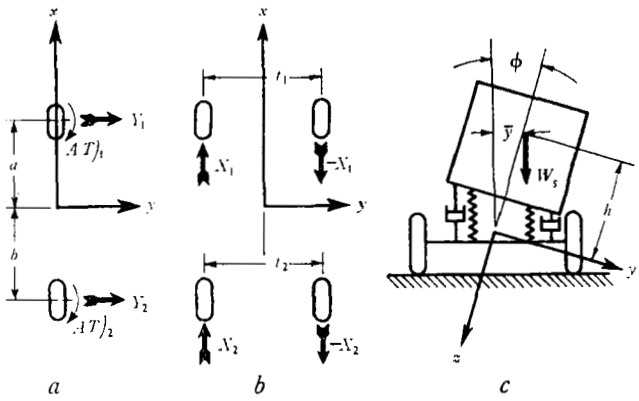


*Fig. 8. Forces and Moments Acting on a Simplified Automobile*

Furthermore, the front and rear slip angles, $\alpha_1$ and $\alpha_2$, can be expressed in terms of the independent variables of motion. If small perturbations are assumed, the front and rear slip angles can be expressed as shown in Fig. 9. In this figure, it should be noted that $\epsilon_2 = \partial\delta_2/\partial\phi$, and is the 'rear roll steer' as determined by geometric properties of the rear suspension. The resulting equations for front and rear tyre slip angles are:

$$\alpha_1 = \beta+\frac{ar}{V}-\delta \quad . \quad . \quad . \quad . \quad (21)$$

$$\alpha_2 = \beta-\frac{br}{V}-\epsilon_2\phi \quad . \quad . \quad . \quad (22)$$

The front and rear load transfer terms, $\Delta Z_1$ and $\Delta Z_2$, are also expressible in terms of the independent variables of motion. For example, the load-transfer quantity, $\Delta Z_2$, can be determined by considering the forces and moments acting on the rear suspension of the automobile. In Fig. 10, the indicated moments, $-(\partial L/\partial p)_2$ and $-k_2\phi$, are those resulting from positive rolling and displacement of the rolling mass as caused by the rear shock absorber and rear suspension roll stiffness, respectively. (The minus signs are necessary since the quantities $\partial L/\partial p$ and $k$ were previously defined with respect to forces acting on the rolling mass). The force $Y'_2$ is the inertia reaction acting at the hypothetical pin joint between the rolling and non-rolling masses. If the inertia of the unsprung mass is neglected in comparison to the rolling mass, then this force, $Y'_2$, is equal and opposite to $Y_2$, the force acting on the tyre by the road. If

$$Y'_2 = -Y_2,$$

the following result is obtained for the rear load transfer by taking moments about point B:

$$\Delta Z_2 = \frac{1}{t_2}\left[Y_2z_2+k_2\phi+\left(\frac{\partial L}{\partial p}\right)_2 p\right] \quad . \quad (23)$$

In a like manner, the incremental vertical load on the front tyres is found to be

$$\Delta Z_1 = \frac{1}{t_1}\left[Y_1z_1+k_1\phi+\left(\frac{\partial L}{\partial p}\right)_1 p\right] \quad . \quad . \quad (24)$$

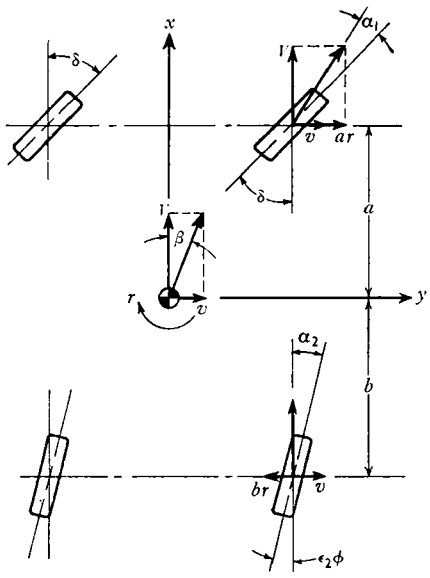


$$\beta_1 = \frac{v+ar}{V} = \beta+\frac{ar}{V}$$

$$\alpha_1 = \beta_1-\delta.$$

$$\beta_2 = \frac{v-br}{V} = \beta-\frac{br}{V}$$

$$\alpha_2 = \beta_2-\epsilon_2\phi.$$

*Fig. 9. Tyre Slip Angles Produced by Vehicle Motion*

From equations (12), (13), (21), and (22) it is seen that

$$Y_1 = C_1\left(\beta+\frac{a}{V}r-\delta\right)+\frac{\partial Y_1}{\partial\phi}\phi \quad . \quad . \quad (25)$$

$$Y_2 = C_2\left(\beta-\frac{b}{V}r-\epsilon_2\phi\right) \quad . \quad . \quad . \quad (26)$$

Substituting (25) and (26) in equations (23) and (24), the following equations for front and rear load transfer are obtained:

$$\Delta Z_1 = \frac{1}{t_1}\left[z_1C_1\left(\beta+\frac{a}{V}r-\delta\right)+z_1\frac{\partial Y_1}{\partial\phi}\phi+k_1\phi+\left(\frac{\partial L}{\partial p}\right)_1 p\right] \quad . \quad . \quad . \quad (27)$$

$$\Delta Z_2 = \frac{1}{t_2}\left[z_2C_2\left(\beta-\frac{b}{V}r-\epsilon_2\phi\right)+k_2\phi+\left(\frac{\partial L}{\partial p}\right)_2 p\right] \quad . \quad (28)$$

If equations (12) through (22), (27), and (28) are substituted in the external force and moment summations given by equations (9), (10), and (11), lengthy and complex relationships are obtained which can be represented functionally as follows:

$$\Sigma Y = f(\beta, r, \delta, \phi) \quad . \quad . \quad . \quad . \quad (29)$$

$$\Sigma N = f(\beta, r, \delta, \phi, p) \quad . \quad . \quad . \quad (30)$$

$$\Sigma L = f(p, \phi) \quad . \quad . \quad . \quad . \quad . \quad (31)$$

These functional relationships can be greatly systematized and abbreviated by use of derivative notation. Thus, equations (29), (30), and (31), when expanded, can be expressed as:

$$\Sigma Y = \frac{\partial Y}{\partial\beta}\beta+\frac{\partial Y}{\partial r}r+\frac{\partial Y}{\partial\delta}\delta+\frac{\partial Y}{\partial\phi}\phi \quad . \quad . \quad . \quad (32)$$

$$\Sigma N = \frac{\partial N}{\partial\beta}\beta+\frac{\partial N}{\partial r}r+\frac{\partial N}{\partial\delta}\delta+\frac{\partial N}{\partial\phi}\phi+\frac{\partial N}{\partial p}p \quad . \quad (33)$$

$$\Sigma L = \frac{\partial L}{\partial p}p+\frac{\partial L}{\partial\phi}\phi \quad . \quad . \quad . \quad . \quad . \quad . \quad . \quad (34)$$

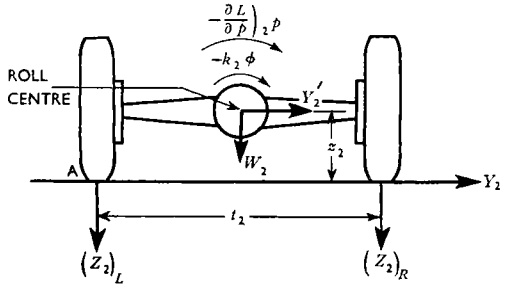


*Fig. 10. Forces and Moments Acting on the Rear Axle and Wheel Assembly*

## The Dimensional Equations of Motion

If an alternative notation is used, $\left(Y_\beta = \frac{\partial Y}{\partial\beta}, \text{ etc.}\right)$, the dimensional equations of motion of an automobile can be expressed as:

$$MV(\dot\beta+r)+M_shp = Y_\beta\beta+Y_rr+Y_\delta\delta+Y_\phi\phi \quad . \quad . \quad (35)$$

$$I_z\dot r+I_{xz}\dot p = N_\beta\beta+N_rr+N_\delta\delta+N_\phi\phi+N_pp \quad . \quad . \quad (36)$$

$$I_x\dot p+M_shV(\dot\beta+r)+I_{xz}\dot r = L_pp+L_\phi\phi \quad . \quad . \quad . \quad . \quad (37)$$

where

$$Y_\beta = C_1+C_2 = C$$

$$Y_r = C_1\frac{a}{V}-C_2\frac{b}{V}$$

$$Y_\delta = -C_1$$

$$Y_\phi = -\epsilon_2 C_2+\frac{\partial Y_1}{\partial \phi}$$

$$N_\beta = aC_1-bC_2+\frac{\partial AT}{\partial \alpha_1}+\frac{\partial AT}{\partial \alpha_2}+\frac{\partial X}{\partial Z}(C_1z_1+C_2z_2)$$

$$N_r = C_1\frac{a^2}{V}+C_2\frac{b^2}{V}+\frac{\partial AT}{\partial \alpha_1}\frac{a}{V}-\frac{\partial AT}{\partial \alpha_2}\frac{b}{V}+\frac{\partial X}{\partial Z}\left(\frac{z_1C_1a}{V}-\frac{z_2C_2b}{V}\right)$$

$$N_\delta = -aC_1-\frac{\partial AT}{\partial \alpha_1}-\frac{\partial X}{\partial Z}z_1C_1$$

$$N_\phi = b\epsilon_2C_2-\frac{\partial AT}{\partial \alpha_2}\epsilon_2+a\frac{\partial Y_1}{\partial \phi}-\frac{\partial X}{\partial Z}\left(z_2C_2\epsilon_2-k-z_1\frac{\partial Y_1}{\partial \phi}\right)$$

$$N_p = \frac{\partial X}{\partial Z}L_p$$

$$L_p = \frac{\partial L}{\partial p}\Big)_1+\frac{\partial L}{\partial p}\Big)_2$$

$$L_\phi = W_sh+k_1+k_2 = W_sh+k$$

The use of the stability-derivative concept to express the external forces and moments acting on an automotive vehicle may be further clarified by an examination of the forces and moments that arise when the car is experiencing motion in one degree of freedom only. Consider, for example, the automobile to be side-slipping to the right, as is indicated in Fig. 11. (For simplicity, incremental drag forces resulting from load transfer have been omitted.) Since $C = \partial Y/\partial \alpha$ is a negative quantity by definition, because of the choice of axis system, a force to the left appears when the car possesses a lateral velocity along the positive $y$ axis. This force always opposes the motion and thus $Y_\beta$ may be considered a damping derivative.

The direction of the yawing moment produced by the cornering forces, however, is critically dependent on the c.g. location and the relative magnitude of the front and rear cornering powers. Forward c.g. locations and rear cornering power higher than front cornering power result in a positive yawing moment for a positive angle of side-slip, while the reverse is true for rearward c.g. locations and low values of rear cornering power relative to front cornering power. (Note that pneumatic trail has the effect of moving the c.g. forward with respect to the tyre reactions, and thereby produces a positive yawing moment. It is more convenient, however, to show tyre forces at the wheel centre and introduce a corresponding aligning torque.)

If the total yawing moment produced by side-slipping is such as to reduce the angle of side-slip, the vehicle may be said to be directionally stable and if the total yawing moment is such as to increase the angle of side-slip, the vehicle may be said to be directionally unstable. The stability derivative $N_\beta$ is thus called the 'directional stability' or the 'directional stiffness'. It is seen that this stability is identical to the weathercocking stability of a weathervane or the directional stability provided by the vertical tail on an aeroplane. In the case of a four-wheeled vehicle, the rear tyres provide a stabilizing moment, while the front tyres provide a destabilizing moment. Note that this attitude stability is merely a property of a vehicle which is side-slipping. While $N_\beta$ does influence the dynamic behaviour, it does not provide positive indication of dynamic stability.

In a similar fashion, the remaining stability derivatives possess physical significance. Thus $Y_\delta$ and $N_\delta$, which are

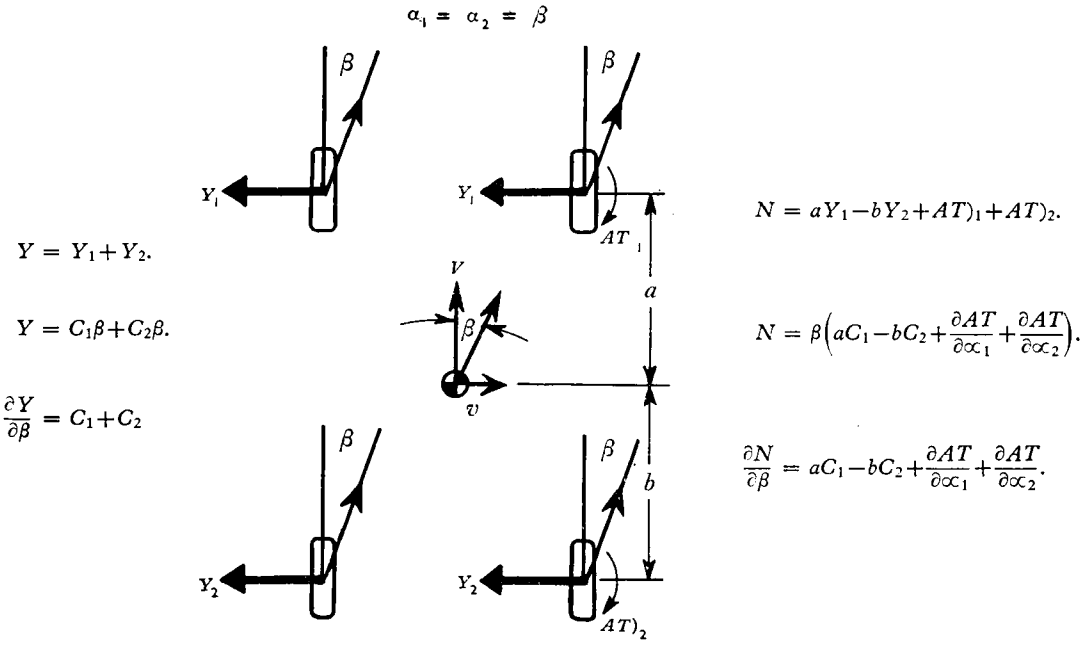


*Fig. 11. Side Force and Yawing Moment Created by a Side-slipping Vehicle*

the side-force and yawing moment produced per unit steering angle of the front wheels, are the 'control effectiveness' derivatives. Increases in $Y_\delta$ and $N_\delta$ alone will increase the response of the vehicle to steering inputs. The derivatives, $Y_\phi$ and $N_\phi$, are essentially 'roll and camber steer' derivatives, in which side-force and yawing moments are produced proportional to (1) the roll-steer properties of the rear suspension, and (2) the camber angle of the front wheels caused by roll of the rolling mass. Since in the steady-state turn a fixed roll angle is produced along with the resultant angle of side-slip, the derivative, $N_\phi$, has directional stability properties similar to $N_\beta$. The derivatives, $L_\phi$ and $L_p$, determine the rolling behaviour of the car and are properly termed the 'roll stiffness' and 'damping-in-roll'. Finally, one of the more important derivatives is $N_r$, the 'damping-in-yaw'. The yawing moment produced by yawing velocity always opposes this angular velocity, as shown in Fig. 12. Note that the front and rear aligning torques are in opposite directions and, hence, tend to cancel one another. The yawing moment produced by the resultant cornering forces is a negative moment for a positive yawing velocity, $r$. Since the induced slip angles at the front and rear tyres are inversely proportional to the forward velocity, $V$, the damping-in-yaw, $N_r$, decreases as forward velocity increases. It is also seen that increasing the wheel base is an effective means of increasing the damping-in-yaw.

A numerical evaluation of the stability derivatives, for the test vehicle used in this study, has shown that certain terms are quantitatively negligible. Although all terms in the static directional stability, $N_\beta$, must be retained, those terms in the yaw damping derivative, $N_r$, caused by aligning torque and load transfer may be neglected. Certain simplifications take place in $N_\delta$ and $N_\phi$ as well. The derivative $N_p$ results only from consideration of the effects of load transfer and does not appear to be important enough to retain in the equations of motion.

## The Non-dimensional Equations of Motion

The utility of the derivatives for comparing the stability characteristics of various vehicles, regardless of physical differences, is considerably enhanced through non-dimensionalization of the above derived equations of motion. In the non-dimensionalization scheme selected as having the most merit, the side-force equation was divided by the total weight of the vehicle and the moment equations were divided by the product of the weight and the wheelbase.

The resulting non-dimensional equations of motion deal with force and moment coefficients together with non-dimensional velocities rather than with absolute forces, moments, and velocities. For example, $\hat{r}$ is the non-dimensionalized form of the yawing velocity, $r$. The non-dimensionalized derivative is indicated by a lower case letter (for example the side-force coefficient produced by side-slipping is $y_\beta$.) Also, with this scheme, the two parameters, $\mu$ and $\tau$, are obtained. The former proves to be the Froude number and may be considered as the non-dimensionalized value of forward velocity, or as the ratio between the inertia and gravitational forces of the system. The second parameter, $\tau$, is a dimensional time constant

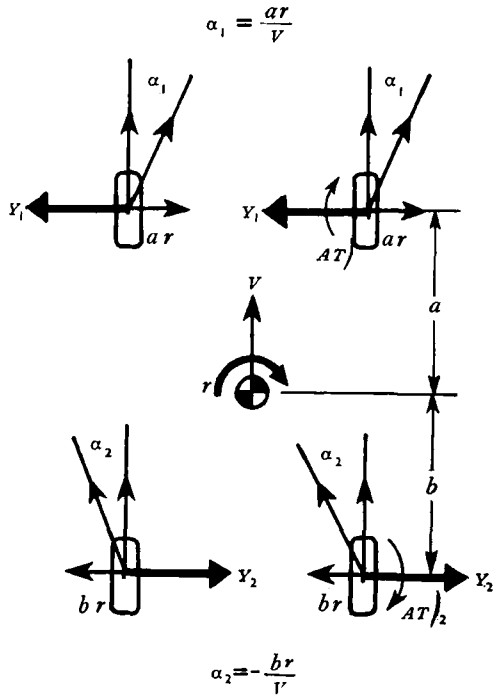


$$Y_1 = C_1\frac{ar}{V}$$

$$AT)_1 = \frac{\partial AT}{\partial \alpha_1}\frac{ar}{V}$$

$$N = \left(C_1\frac{a^2}{V} + C_2\frac{b^2}{V} + \frac{\partial AT}{\partial \alpha_1}\frac{a}{V} - \frac{\partial AT}{\partial \alpha_2}\frac{b}{V}\right)r$$

$$Y_2 = -C_2\frac{br}{V}$$

$$AT)_2 = -\frac{\partial AT}{\partial \alpha_2}\frac{br}{V}$$

*Fig. 12. Yawing Moment Produced by Yawing Velocity*

that conveniently removes time from the dimensional equations. Further, the moments of inertia reduce to their respective radii of gyration ratioed to the reference-length parameter which is the wheelbase, $l$.

Accordingly, the non-dimensional equations of motion, with the input forces and moments placed on the right-hand side, are:

Side-force equation

$$(\mu D-y_\beta)\beta+(\mu-y_r)\hat{r}+(mD^2-y_\phi)\phi = y_\delta\delta \quad (38)$$

Yawing moment equation

$$(-n_\beta)\beta+(i_zD-n_r)\hat{r}+(i_{xz}D^2-n_\phi)\phi = n_\delta\delta \quad (39)$$

Rolling moment equation

$$(m\mu D)\beta+(i_{xz}D+m\mu)\hat{r}+(i_xD^2-l_pD-l_\phi)\phi = 0 \quad (40)$$

where

$$\tau = \sqrt{l/g}$$

$$D = \tau\frac{d}{dt}$$

$$\hat{r} = \tau r$$

$$\mu = V/\sqrt{lg}$$

$$m = \frac{M_s h}{Ml}$$

$$i_{xz} = \frac{M_s hc}{Ml^2}$$

$$i_x = \frac{I_x}{Ml^2}$$

$$i_z = \frac{I_z}{Ml^2} = \left(\frac{k_z}{l}\right)^2$$

$$y_\beta = \frac{Y_\beta}{Mg} = \frac{C}{Mg}$$

$$y_r = \frac{Y_r}{M\sqrt{lg}} = -\frac{C}{Mg}\frac{1}{\mu}\left(\frac{C_2}{C}-\frac{a}{l}\right)$$

$$y_\phi = \frac{Y_\phi}{Mg} = -\frac{C}{Mg}\left(\epsilon_2\frac{C_2}{C}-\frac{\partial Y_1/\partial\phi}{C}\right)$$

$$y_\delta = \frac{Y_\delta}{Mg} = -\frac{C}{Mg}\left(1-\frac{C_2}{C}\right)$$

$$n_\beta = \frac{N_\beta}{Mlg} = -\frac{C}{Mg}\left[\frac{C_2}{C}-\frac{a}{l}-\frac{\partial AT/\partial\alpha_1+\partial AT/\partial\alpha_2}{Cl} - \frac{\partial X}{\partial Z}\left(\frac{z_1}{l}+\frac{z_2-z_1}{l}\frac{C_2}{C}\right)\right]$$

$$n_r = \frac{N_r}{Ml\sqrt{lg}} = -\frac{1}{\mu}\frac{C}{Mg}\left[\frac{C_2}{C}\left(\frac{2a}{l}-1\right)-\left(\frac{a}{l}\right)^2\right]$$

$$n_\phi = \frac{N_\phi}{Mlg} = -\frac{C}{Mg}\left(-\frac{C_2}{C}\epsilon_2\frac{b}{l}-\frac{a}{l}\frac{\partial Y_1/\partial\phi}{C}-\frac{\partial X}{\partial Z}\frac{k}{Cl}\right)$$

$$n_\delta = \frac{N_\delta}{Mlg} = -\frac{C}{Mg}\left[\frac{a}{l}\left(1-\frac{C_2}{C}\right)+\frac{\partial AT/\partial\alpha_1}{Cl}\right]$$

$$l_p = \frac{\mathscr{L}_p}{Ml\sqrt{lg}}$$

$$l_\phi = \frac{L_\phi}{Mlg} = \frac{W_s h+k}{Mlg}$$

In this listing of the non-dimensional stability derivatives, three physically significant parameters appear again and again. These are:

(1) the total cornering coefficient of the vehicle, $-C/Mg$
(2) the centre-of-gravity location, $a/l$, and
(3) the ratio of rear to total cornering power, $C_2/C$.

While stability parameters such as rear roll steer, $\epsilon_2$, front wheel camber thrust, $\partial Y_1/\partial\phi$, etc., do have an appreciable influence on the directional behaviour of an automotive vehicle, the basic stability parameters of an automobile, exclusive of its mass and inertia characteristics, are these three quantities. An examination of all the constants appearing in the equations of motion reveals that a total of twenty properties of the simplified automobile must be known in order to predict its dynamic lateral motions. These properties fall into the following three categories:

(1) mass and inertia characteristics,
(2) chassis or suspension properties, and
(3) tyre characteristics.

## Solution of the Equations of Motion

To compute the response to front-wheel angle inputs, the derived equations of motion must be solved simultaneously by either classical or operational methods. Since the derived equations are linear differential equations with constant coefficients, the techniques of operational calculus are particularly suited for this task. If the automobile is assumed to possess zero initial lateral motion, application of the Laplace transform to equations (38), (39), and (40), in accordance with the procedure described in Gardner and Barnes,[180] yields

$$\begin{bmatrix} \mu s-y_\beta & \mu-y_r & ms^2-y_\phi \\ -n_\beta & i_z s-n_r & i_{xz}s^2-n_\phi \\ m\mu s & i_{xz}s+m\mu & i_x s^2-l_p s-l_\phi \end{bmatrix}\begin{bmatrix} \beta(s) \\ \hat{r}(s) \\ \phi(s) \end{bmatrix} = \begin{bmatrix} y_\delta\delta(s) \\ n_\delta\delta(s) \\ 0 \end{bmatrix} \quad (41)$$

The solution of the original differential equations has now been reduced to the solution of a set of algebraic equations. If determinants are used, the solution for $\beta(s)$, for example, becomes

$$\beta(s) = \frac{\begin{vmatrix} y_\delta & \mu-y_r & ms^2-y_\phi \\ n_\delta & i_z s-n_r & i_{xz}s^2-n_\phi \\ 0 & i_{xz}s+m\mu & i_x s^2-l_p s-l_\phi \end{vmatrix}}{\begin{vmatrix} \mu s-y_\beta & \mu-y_r & ms^2-y_\phi \\ -n_\beta & i_z s-n_r & i_{xz}s^2-n_\phi \\ m\mu s & i_{xz}s+m\mu & i_x s^2-l_p s-l_\phi \end{vmatrix}}\delta(s) \quad (42)$$

The time response of $\beta$ is found upon application of the inverse Laplace tranformation. Thus,

$$\beta\left(\frac{t}{\tau}\right) = \mathscr{L}^{-1}[\beta(s)] \quad . \quad . \quad . \quad (43)$$

where $\mathscr{L}^{-1}$ is the symbol for the inverse Laplace transformation.

Similarly, the steady-state response of a vehicle to a sinusoidal input of front-wheel angle, $\delta$, is obtained by replacing the Laplace argument, $s$, by the quantity, $j\omega\tau$,

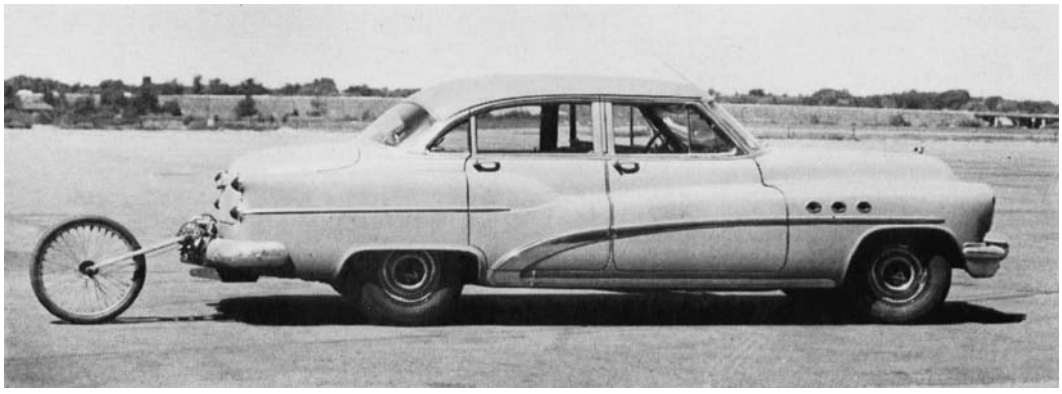

*Fig. 13. Buick Test Car*

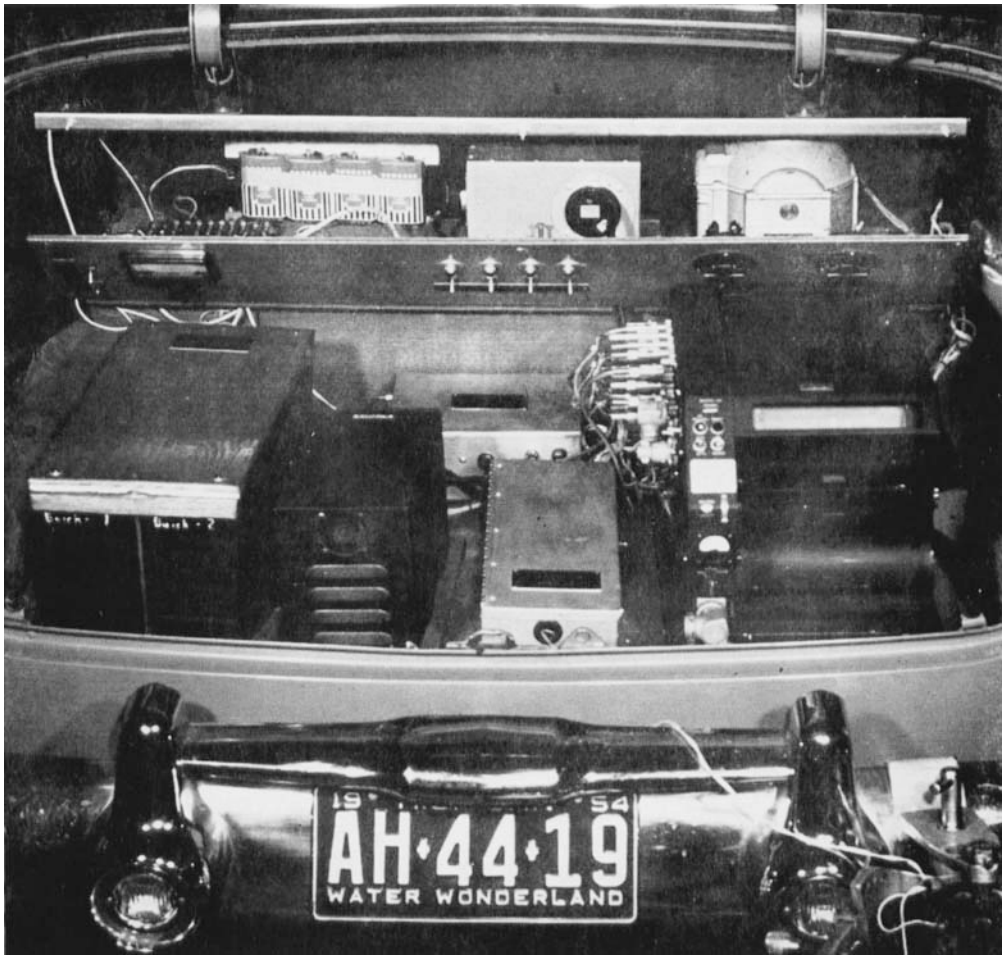


*Fig. 29. Instrumentation Installation in Trunk of Test Car*

where $\omega\tau$ is the non-dimensional circular frequency. This steady-state response is called the frequency response. For example, the yawing-velocity frequency response is expressed as follows:

$$\frac{\hat{r}(j\omega\tau)}{\delta(j\omega\tau)} = \frac{\begin{vmatrix} \mu j\omega\tau - y_\beta & y_\delta & -m(\omega\tau)^2 - y_\phi \\ -n_\beta & n_\delta & -i_{xz}(\omega\tau)^2 - n_\phi \\ m\mu j\omega\tau & 0 & -i_x(\omega\tau)^2 - l_p j\omega\tau - l_\phi \end{vmatrix}}{\begin{vmatrix} \mu j\omega\tau - y_\beta & \mu - y_r & -m(\omega\tau)^2 - y_\phi \\ -n_\beta & i_z j\omega\tau - n_r & -i_{xz}(\omega\tau)^2 - n_\phi \\ m\mu j\omega\tau & i_{xz} j\omega\tau + m\mu & -i_x(\omega\tau)^2 - l_p j\omega\tau - l_\phi \end{vmatrix}} \quad (44)$$

## EXPERIMENTAL SUBSTANTIATION OF THE LEVEL ROAD, FIXED-CONTROL EQUATIONS

### Stability Parameter Measurements

The test vehicle used in this investigation was the 1953 Buick Super, four-door Sedan pictured in Fig. 13, Plate 1. Since substantiation of the derived mathematical model is accomplished by comparing experimental data with theoretically computed responses, it was necessary that a test programme be performed to evaluate the stability parameters of the Buick. To this end, the yawing and rolling moments of inertia were measured at C.A.L. by respectively swinging the car as a multifilar pendulum and oscillating it in roll on its rear suspension springs. The total weight and longitudinal location of the c.g. of the instrumented car were determined by weighing, with the non-rolling mass assumed to be the rear unsprung mass, the weight of which was supplied by the General Motors Corporation (G.M.).

Data on the physical and geometrical properties of the suspension of the test vehicle were evaluated jointly by C.A.L. and G.M. The necessary tests yielded the roll spring rate, rear roll steer, roll damping, front-wheel camber due to body roll, and height of the front and rear roll centres.

The most important parameters contained in the definition of the stability derivatives of an automobile are the lateral force and moment characteristics of the pneumatic tyre. The functional relationship between lateral tyre properties and the primary independent variables (that is, slip-angle, camber angle, and loading) have been defined in an empirical manner, since, unfortunately, no integrated theory of tyre mechanics exists to predict the mechanical behaviour of a tyre as a function of its construction, size, pressure, loading, slip-angle, etc. In addition, tyres, like other mechanical systems, possess dynamic as well as static or steady-state properties. It is found, however, that very little information is available on lateral dynamic behaviour of tyres.

In this investigation, the steady-state properties of the tyres used on the test vehicle were supplied by the United States Rubber Company, who performed the necessary tests with their rolling drum equipment. These drum results were arbitrarily increased in accordance with data presented by Bull[98] in an effort to obtain data which would be valid for a tyre operating on a flat surface. Although tyre dynamics, or lag in tyre-force build up, does have some influence on the response of an automobile, this effect was neglected in developing the described mathematical model. Since this is a subject in itself, full discussion of this point is not presented herein. Instead, it is demonstrated that the effects of tyre dynamics are small in the particular frequency range that characterizes the rigid-body motions of the automobile.

### Response Test Methods

The test car was instrumented to permit dynamic recording of the nine variables listed in Table 1. Both left and right front-wheel positions were recorded and averaged to yield the effective front-wheel angle $\delta$. Since it is not convenient to measure side-slip or lateral velocity, the total lateral acceleration along the $y$ axis was measured with a lateral accelerometer. This acceleration is denoted by the symbol, $n_y$, and is composed of the linear acceleration, $\dot{v}$, the centrifugal acceleration, $Vr$, and a component of gravity caused by the roll angle, $\phi$. The pitch attitude, $\theta$, as listed in Table 1, is not a lateral degree of freedom, but its measurement was made to check any coupling that might have occurred between the longitudinal and lateral motions. Listed also in Table 1 are the sensing instruments or transducers that were used to convert each variable to an appropriate electrical signal for recording on an 18-channel G.E.C. oscillograph. Additional details on the instrumentation of the test car are presented in Appendix IV.

*Table 1. Measured Variables and Associated Transducers*

| Variable of motion | Sensing instrument |
|---|---|
| Left front wheel position, $\delta_L$ | Angular potentiometer |
| Right front wheel position, $\delta_R$ | Angular potentiometer |
| Steering wheel position, $\delta_s$ | Angular potentiometer |
| Lateral acceleration, $n_y$ | Statham lateral accelerometer |
| Roll attitude, $\phi$ | Minneapolis-Honeywell attitude gyro |
| Pitch attitude, $\theta$ | Minneapolis-Honeywell attitude gyro |
| Angular yaw velocity, $r$ | Doelcam rate gyro |
| Angular roll velocity, $p$ | Doelcam rate gyro |
| Forward velocity, $V$ | Fifth wheel generator set |

Fig. 14 is a block representation of the recording circuitry installed in the test vehicle. It is seen that the oscillograph trace deflexion is a function of the response of the automobile as modified by the dynamics of a given recording

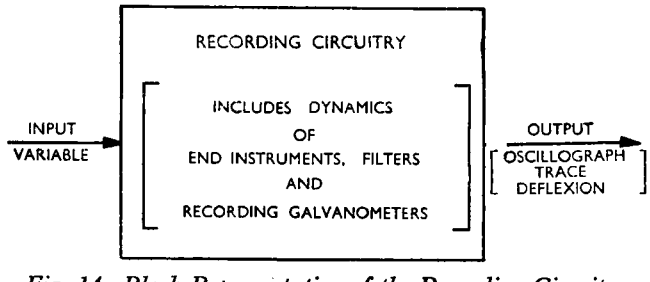


*Fig. 14. Block Representation of the Recording Circuitry*

channel. This result requires that the effects of the recording circuitry 'block' be removed, in order to obtain a true picture of the response of the car. For this reason, the measured transient responses of the car were harmonically analysed to yield the frequency response of the automobile plus that of the recording circuitry. The frequency response of the car alone was obtained by removing the dynamics of the recording equipment from the results of the harmonic analysis.

A second reason for reducing the measured time histories to frequency-response form is that measured frequency responses can be compared with theoretically computed responses irrespective of the manoeuvre performed and the actual shape of the applied steering-wheel displacement. Since a dynamic system can be described either in terms of its transient response to a given input or in terms of its steady-state response to an applied sinusoidal input, it is possible to compare theory and experiment in either the time or frequency plane. In this particular task, both instrumentation and testing considerations required the use of the well-proved 'frequency-response technique'.

The initial phase of the test programme was devoted to measurement of the steady-state response of the Buick. Tests were made at forward speeds of approximately 15, 30, 45 and 60 m.p.h. on runways of the Buffalo Municipal Airport. The primary purpose of the steady-state tests was to obtain static or steady-state response information for all stability configurations in which the dynamic response was to be measured. While the skid-pad test, as developed by G.M., had previously indicated the range of lateral acceleration over which the automobile could be treated as a linear system, a need still existed for correlating the steady-state response in this range with predictions based upon linear tyre data and linear equations of motion.

The steady-state tests were made in the following manner. The forward velocity was stabilized at the desired speed with the test car proceeding straight down the runway. Shortly after the recording switch was turned on, the steering wheel was turned to a new position and held there while the car proceeded into a steady turn configuration. When the steady state was reached, the recording was stopped and a recovery was made to prevent running off the runway.

Transient responses of the Buick to step and pulse inputs of front-wheel angle were measured in the dynamic phase of the test programme. In a procedure similar to that followed in the steady-state response tests, the car was stabilized at a given speed, the control motion executed, and the recording continued until the steady state was reached. Fig. 15 shows the transient response of the Buick to a pulse input of front-wheel angle as obtained during a typical transient test manoeuvre. Response time histories such as these were harmonically analysed with the aid of a rolling-sphere-type mechanical harmonic analyser. The harmonic content of the output or response variables was ratioed to the harmonic content of the front-wheel angle trace, and yielded the frequency response of the automobile plus that of the recording circuitry. Final amplitude- and phase-response data were obtained by correcting for the effects of the recording equipment.

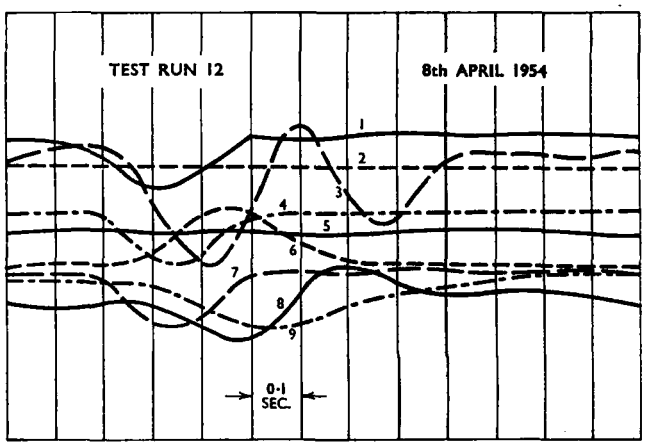


*Fig. 15. Transient Response of Buick to Pulse Input of Front-wheel Angle*

1. Steering wheel position, $\delta_{SW}$.
2. Forward velocity, $V$.
3. Lateral acceleration, $n_y$.
4. Left front wheel, $\delta_L$.
5. Pitch attitude, $\theta$.
6. Yaw rate, $r$.
7. Right front wheel, $\delta_R$.
8. Roll rate, $p$.
9. Roll angle, $\phi$.

To substantiate the theory as extensively as possible, response data were obtained for as wide a range of stability conditions as was practical. Data were therefore obtained in tests wherein the following stability parameters were varied:

(1) Forward velocity, $V$,
(2) Directional stability, $N_\beta$,
(3) Roll stiffness, $L_\phi$, and
(4) Total cornering coefficient, $C/Mg$.

Variations in the directional stability were achieved by moving the centre of gravity of the test vehicle and varying tyre pressures front and rear. A roll-stiffness modification was achieved by disconnecting the roll stabilizer bar and a major change in total cornering coefficient was obtained by raising all tyre pressures from 24 to 40 lb. per sq. in.

## Comparison of Theory and Experiment

The three lateral degrees of freedom considered in the mathematical model are:

(1) lateral displacement, velocity, or acceleration along the $y$ axis,
(2) angular displacement, velocity, or acceleration around the $z$ axis, and
(3) angular displacement, velocity, or acceleration around the $x$ axis.

It should be noted that the first two are primarily directional degrees of freedom, whereas the third influences the directional behaviour only through the roll-steer properties of the chassis, and the effects of inertia coupling. None the less, a complete check of the theory can be obtained only by measuring all three lateral degrees of freedom, and comparing the response in each degree of freedom to that

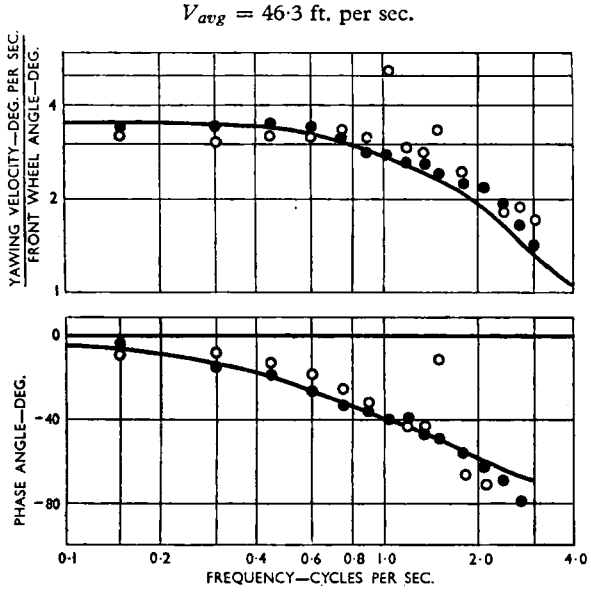


*Fig. 16. Calculated and Experimental Frequency Response —Yawing Velocity*

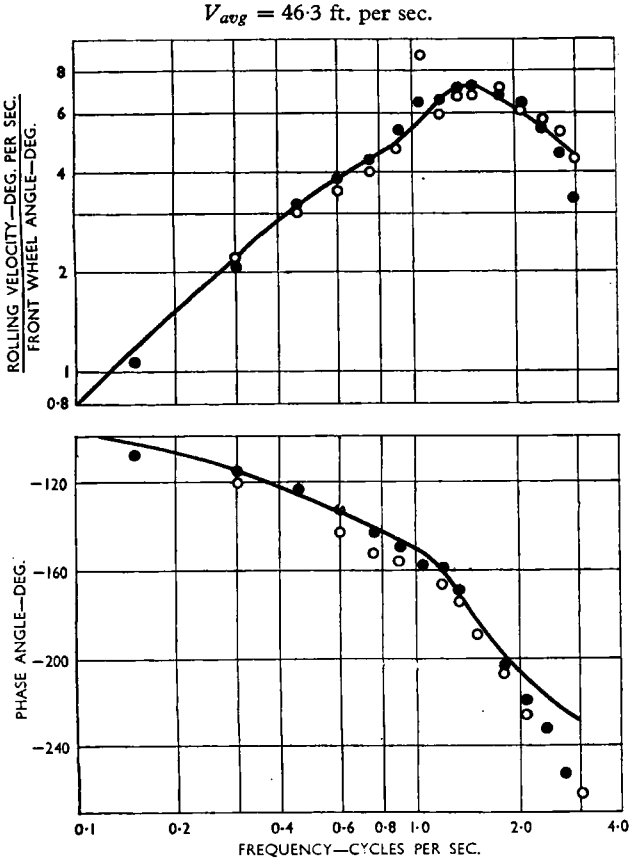


*Fig. 17. Calculated and Experimental Frequency Response —Rolling Velocity*

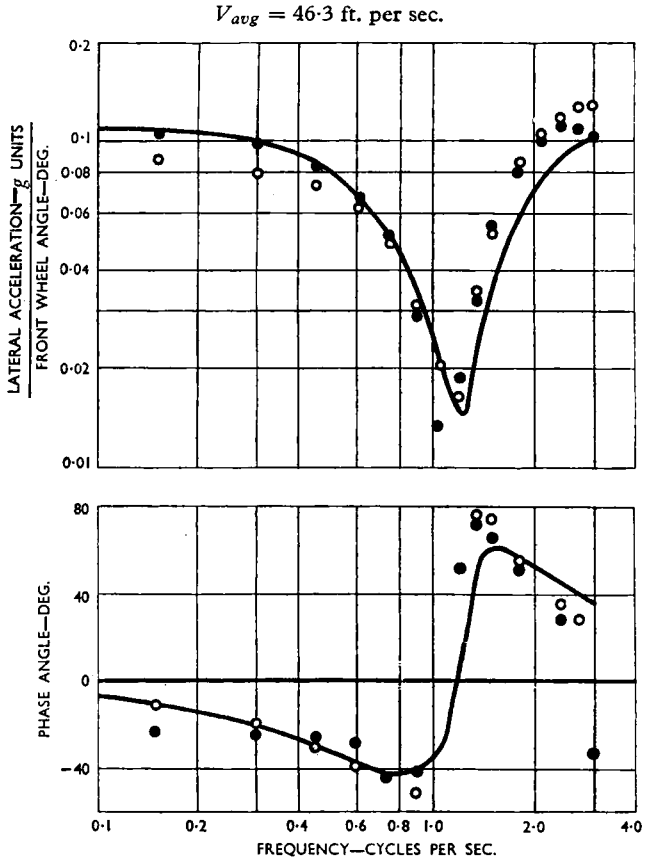


*Fig. 18. Calculated and Experimental Frequency Response —Lateral Accelerations*

predicted by theory. It was on the basis of this premise that the dynamic response tests described herein were planned and performed.

Figs. 16, 17, and 18 present the results of the harmonic analysis of the response data obtained with the Buick in the standard-instrumented test configuration. (In this configuration, the c.g. was located 51·7 per cent of the wheelbase aft of the front wheel centre and the tyre pressures were 24 lb. per sq. in. front and rear). The solid lines on these plots are the theoretically predicted responses yielded by the derived equations of motion. It is seen that good-to-excellent agreement exists between theory and experiment for all three degrees of freedom.

The resultant yawing velocities at the low end of the frequency spectrum are primarily a function of the directional stiffness (Fig. 16). As $f$ increases beyond 2 cycles per sec., the inertia of the system begins to predominate and the yawing velocity response tends to decrease at a rate independent of the directional stiffness of the system. A high-frequency steering input produces very little response and this result certainly agrees with human intuition and experience. In theory, the phase lag between front-wheel angle and yawing velocity approaches 90 deg. with increasing frequency when it is assumed that there is no lag between tyre force and tyre slip angle. In actual practice,

however, tyre dynamics will cause the measured phase lags to increase over and above 90 deg. at high oscillation frequencies.

Fig. 17 demonstrates that $p$ increases with increasing frequency, eventually peaks, and then decreases at a rate which is primarily determined by the rolling moment of inertia. With the assumption that the tyres are devoid of dynamic properties, the phase lag between $p$ and $\delta$ goes from $-90$ to $-270$ deg. as the oscillation frequency is varied from zero to infinity.

The unusual shape of the lateral-acceleration response presented in Fig. 18 is explained by the fact that the acceleration measured by the lateral accelerometer is composed of:

(1) the centrifugal acceleration caused by yawing velocity,
(2) a component of the acceleration of gravity caused by roll of the car body, and
(3) a linear acceleration along the lateral $y$ axis.

The first two of these three components of lateral acceleration exist in the steady state and then decrease with increasing frequency, whereas the third component is zero in the steady state and increases with increasing frequency. Each acceleration component is a vector quantity when considered in the frequency plane and they all add vectorially to produce the amplitude and phase characteristics observed on this figure. Contrary to the yawing and rolling-velocity responses, the lateral acceleration response asymptotically approaches a finite value as the oscillation frequency is increased towards infinity (that is, when tyre dynamics are ignored). Physically, it is readily seen that although there is no yawing velocity or roll-angle response at an infinite oscillation frequency, there must be a side-force produced by the steering of the front wheels. This side-force will, of course, produce a linear acceleration along the $y$ axis. The response, $|n_y/\delta|$, at $f = \infty$, is given by theory as

$$\left|\frac{n_y}{\delta}\right|_{f=\infty} \cong \frac{-C_1}{Mg\left(1-\frac{M_s}{M}\frac{M_s h^2}{I_x}\right)} \quad . \quad . \quad (45)$$

Thus, it is seen that the lateral acceleration response at $f = \infty$ is equal to the front-wheel cornering stiffness divided by the weight of the vehicle as modified by properties of the rolling mass. Positive acceleration is produced by positive $\delta$ and therefore, $\varphi_{n_{y_\delta}} = 0$ at $f = \infty$. Because the phase angle between the acceleration and the front-wheel angle approaches zero with increasing frequency, if tyre dynamics are ignored, this response is particularly suitable for determining the influence of tyre dynamics on the overall vehicle response.

Data similar to those presented in Figs. 16, 17, and 18 were obtained for seven test configurations. When the measured responses were compared with those yielded by the derived equations of motion, it was concluded that the derived mathematical model adequately defines the lateral dynamic behaviour of the fixed-control automobile operating on a level road. It was further concluded that the effects of lag between tyre slip angle and tyre force on the directional response of an automobile are very small at oscillation frequencies below 3 cycles per sec. for forward speeds greater than 15 m.p.h., which is to say, path wave lengths greater than $7\frac{1}{3}$ feet.

## THE RESPONSE OF THE FIXED-CONTROL AUTOMOBILE TO STEERING CONTROL

### Steady-State Response

With the aid of a substantiated mathematical model, it is feasible to examine the steady state and dynamic behaviour of the automobile and to define quantitatively those factors which govern the control and stability characteristics of an automotive vehicle. This task is made practicable by the use of linear equations of motion which can be solved by means of straightforward analytical procedures.

A solution of the equations of motion reveals that the vehicle response to steering inputs is composed of:

(1) a transient response, during which the vehicle experiences angular and lateral accelerations, and
(2) a steady-state response, in which the centrifugal force arising in the steady turn is balanced by the resulting tyre forces.

Experience has shown that it is informative to study the steady-state and transient responses individually. In terms of the frequency response, this is equivalent to studying the response of the vehicle at an oscillation frequency equal to zero and the response at all frequencies other than zero. Vehicle response to a fixed steering input is called the 'static sensitivity' of the vehicle and as such is an important aspect of the overall behaviour of the vehicle. It is this aspect of the stability and control characteristics of the automobile which is examined first.

During a steady turn produced by a fixed displacement of the front wheels, an automobile possesses:

(1) a constant turning rate or yawing velocity,
(2) a fixed roll angle, and
(3) a fixed angle of side-slip.

In the moment equilibrium established in the turn, it is the steering moment, $N_\delta\delta$, that primarily balances the yaw-damping moment, $N_r r$, since the moments caused by side-slip and roll angle are small and often are zero. To repeat, the positive steering moment in a right turn overcomes, in the main, the negative damping-in-yaw moment. If the moments due to side-slip and roll angle are assumed to be zero, the steady-state yawing moment equation yields the following important result for the yawing velocity response per unit front-wheel angle input:

$$\left(\frac{r}{\delta}\right)_{ss} = \frac{V}{l} \quad . \quad . \quad . \quad . \quad . \quad (46)$$

Since $V = Rr$, where $R$ is the radius of the steady turn, it is seen that, under the assumed conditions, the steering angle in a steady turn is equal to $l/R)_{ss}$, which is defined as

the Ackermann angle. Thus, a vehicle without directional stability and roll-steer properties has a yawing-velocity response which is a function of its Ackermann layout. A steady-state yawing-velocity response equal to the forward velocity divided by the wheelbase is the basic response characteristic of the automobile and is modified only by the existence of roll steer and directional stability properties.

On the other hand, an exact solution of the equilibrium equations of motion yields the following equation for the yawing-velocity response:

$$\left(\frac{r}{\delta}\right)_{ss} = \frac{1}{\tau}\left[\frac{y_\delta \frac{n_\beta}{y_\beta} - n_\delta}{n_r + \frac{n_\phi m\mu}{l_\phi} + \frac{n_\beta}{y_\beta}\left(\mu - y_r - \frac{y_\phi m\mu}{l_\phi}\right)}\right] \quad (47)$$

This exact solution can be transformed to the following simplified form:

$$\left(\frac{r}{\delta}\right)_{ss} = \frac{V/l}{1+KV^2} \quad . \quad . \quad . \quad . \quad (48)$$

where

$$K = \frac{1}{lg}\left[\frac{-\frac{n_\beta}{y_\beta} - \frac{mn_\phi}{l_\phi - my_\phi}}{n_\delta - y_\delta \frac{n_\beta}{y_\beta}}{1 - \frac{my_\phi}{l_\phi}}\right] \quad . \quad . \quad (49)$$

Equation (48) shows the manner in which the steady-state yawing-velocity response varies as a function of forward velocity, $K$ being a constant that is independent of velocity. It is seen that the yawing-velocity response is equal to the 'basic response', $V/l$, when the constant $K$ is equal to zero. Examination of equation (49) shows that this equalization will occur when the directional stability, $n_\beta$, and the roll steer moment, $n_\phi$, are equal to zero, as was assumed in the preceding argument.

The numerator of equation (49) thus takes on particular significance. The sign of $K$ can be negative or positive, depending on the sign of both the directional stiffness, $n_\beta$, and the yawing moment due to roll, $n_\phi$. Since $n_\beta$ is the non-dimensional yawing moment due to side-slip, and $y_\beta$ is the non-dimensional side force due to side-slip, the term $n_\beta/-y_\beta$ is the effective non-dimensional distance between the centre of reaction of the tyre forces and the c.g. of the vehicle. It is thus seen that this moment arm, expressed as a percentage of the wheelbase, is an alternative method of defining the directional stability of an automobile. For fixed tyre properties, that is, a fixed position of the reaction centre of the lateral tyre forces caused by side-slipping, this moment arm can be varied by moving the c.g. fore and aft. Similarly, the c.g. can be held fixed and the effective lateral reaction centre of the tyres can be moved along the longitudinal axis by varying tyre cornering stiffness both front and rear. The effective lateral-reaction centre of the tyres has been termed the 'neutral steer point' and this concept is discussed in more detail in subsequent papers by Fonda, and Whitcomb and Milliken. It shall suffice to say here that $n_\beta/-y_\beta$ is the distance between the neutral steer point and the c.g. of a non-rolling vehicle and, as such, represents the directional stiffness or the 'static margin' of a non-rolling vehicle as defined in an earlier paper by Walker.[50]

The second term in the numerator of equation (49) represents a contribution to the static margin of the vehicle by the roll steer and camber thrust effects which may be experienced by a rolling automobile. In the case of an independent front-suspension vehicle, wherein the front wheels camber with body roll, this 'roll' term adds a sizable positive contribution to the static margin of a non-rolling vehicle. The numerator of equation (49) is, thus, the total static margin of an automobile and, as discussed above, is a numerical measure of the total directional stiffness, produced both by moment due to side-slip and moment due to roll angle. Positive static margins are produced by positive values of $n_\beta$ and $n_\phi$, and negative static margins are produced by negative values of $n_\beta$ and $n_\phi$.

To recapitulate, the automobile yawing-velocity response to steering inputs, that is, angular displacement of the front wheels, is basically equivalent to its Ackermann response, $V/l$, as modified by the total directional stiffness of the vehicle, this stiffness being alternatively expressed by the static margin. This statement is expressed mathematically by equations (48) and (49). Fig. 19 shows the manner in which the steady-state yawing-velocity response to front-wheel angle, $\delta$, varies with velocity for a vehicle with positive, zero, and negative static margins. The equation which applies to this figure is, of course, equation (48). Speaking in terms of curvature response rather than yawing-velocity response, Fig. 19 is transformed into Fig. 20, where it is seen that a vehicle with zero static margin is one that has a constant curvature response with increasing

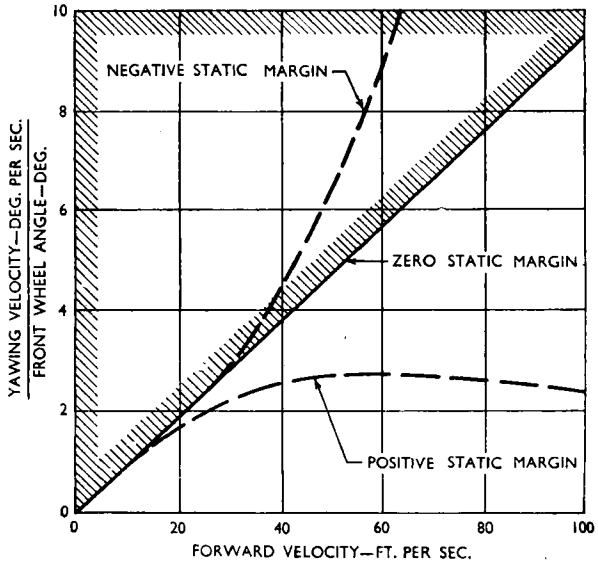


*Fig. 19. Influence of Static Margin on the Steady-state Yawing-velocity Response*

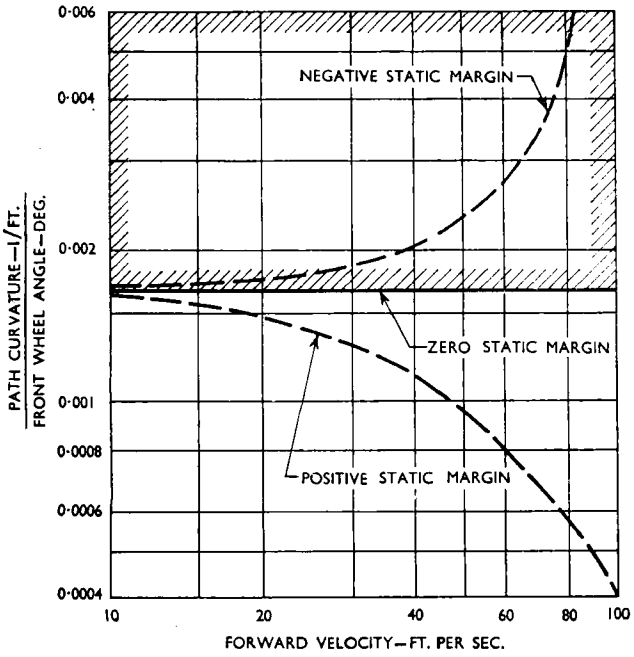


*Fig. 20. Influence of Static Margin on the Steady-state Curvature Response*

forward velocity, and a vehicle with negative static margin has an increasing curvature response with increasing forward velocity.

Both Figs. 19 and 20 indicate that the directional response of an oversteer vehicle increases rapidly as a certain critical speed is reached, because the denominator in equation (48) approaches zero with increasing $V$. If $1+KV^2$ is set equal to zero, it is possible to determine, for a given negative static margin, the velocity at which the steady-state response theoretically becomes infinite, or, for a given $V$, it is possible to determine the negative static margin which makes the response become infinite. Practically speaking, however, the steady-state response, under conditions wherein the quantity $(1+KV^2)$ approaches zero, would never be reached, since the vehicle soon would exceed the side-force capacity of its tyres and would, therefore, go into a skid.

At this point it is desirable to relate 'oversteer' and 'understeer' to the static margin of the automobile. Olley[32, 45] defined understeer and oversteer in terms of the path or course pursued by a straight-running vehicle when subjected to a steady side load applied at the centre of gravity (Fig. 21). If the front and rear side-slip angles are defined as those angles between the longitudinal axis of the car and the velocity vectors of the front and rear axle centres, it is seen that the path of the car is determined by these steady-state side-slip angles. If an applied side load produces equal front and rear side-slip angles, the vehicle moves off on a new straight-line path. A rear side-slip angle greater than the front side-slip angle will result in a curved path toward the applied load, and front side-slip angle greater than rear side-slip angle will result in a

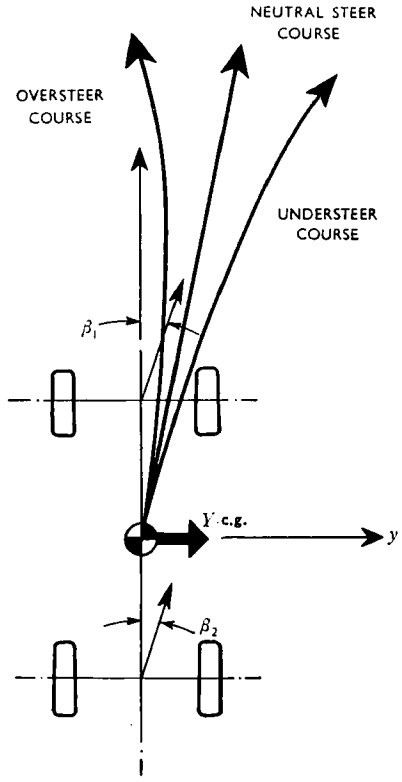


*Fig. 21. Over/Understeer Representation of Vehicle Stability*

curved path away from the applied load. The terms neutral steer, oversteer, and understeer were applied to these three path configurations, in the order named, as indicated in Fig. 21.

In terms of yawing velocity, Fig. 21 may be interpreted as follows:

(1) When the vehicle is neutral-steer, a positive side load at the c.g. produces zero yawing velocity.

(2) When the vehicle is understeer, a positive side load at the c.g. produces a positive yawing velocity.

(3) When the vehicle is oversteer, a positive side load at the c.g. produces a negative yawing velocity.

A solution of the equilibrium equations of motion reveals that the steady-state yawing-velocity response to a force applied along the positive $y$ axis is positive when the static margin is positive. There is no yawing velocity when the static margin is zero. The yawing-velocity response is negative when the static margin is negative. In these definitions of understeer and oversteer, it is seen that an understeer vehicle is one which possesses a positive static margin or positive directional stiffness; an oversteer vehicle possesses a negative static margin or negative directional stiffness.

The above relationship between over/understeer and static margin is also demonstrated by the skid-pad version

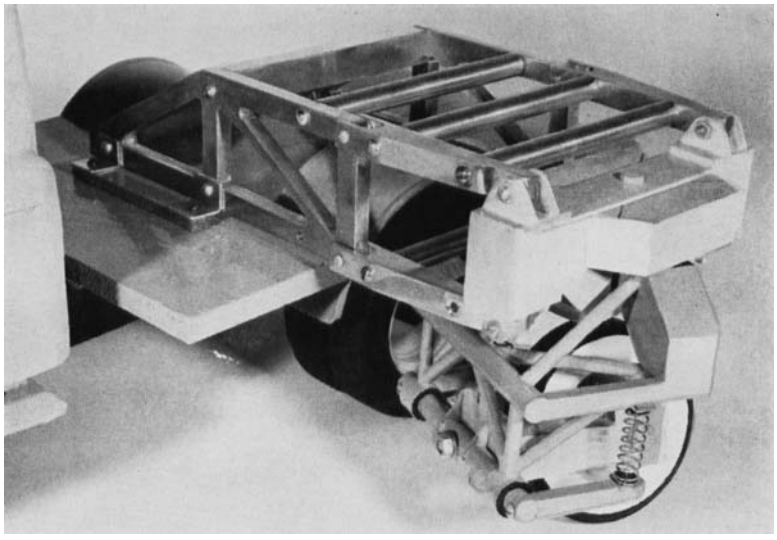

*Fig. 32. Model of Second Design*

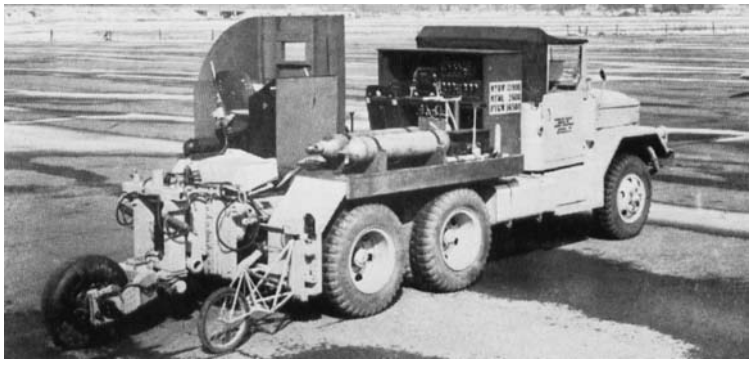

*Fig. 34. General View of Final Configuration*

*Fig. 35. Rear View, Wheel Cambered and Steered*

[I.Mech.E., 1956–57]

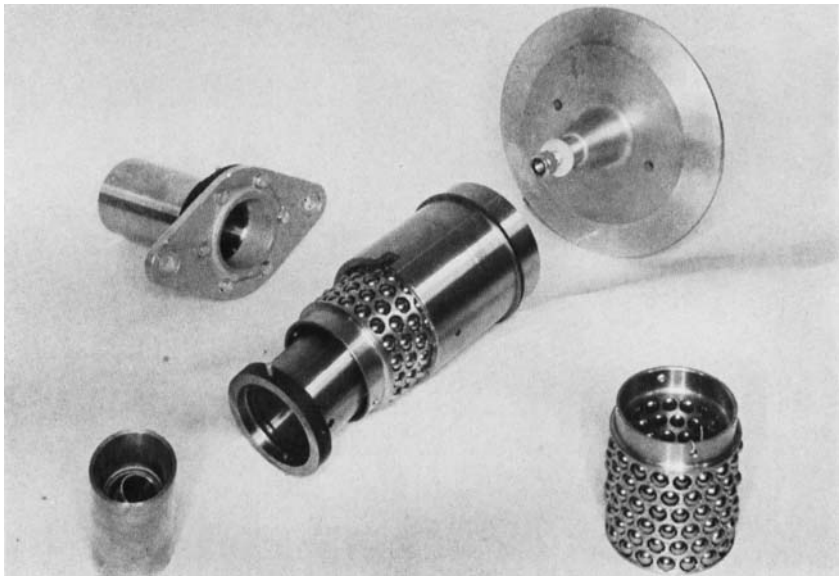

*Fig. 49. Linear Ball Bushings*

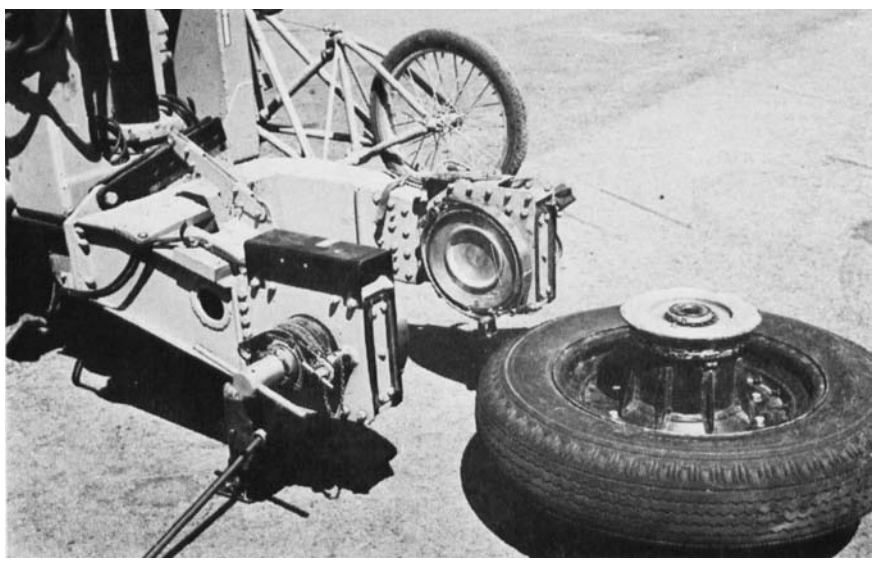

*Fig. 50. Wheel Unit Removed*

of equation (48). On rearranging equation (48), there results:

$$\delta)_{ss} = \frac{l}{R} + K\frac{lV^2}{R} \quad . \quad . \quad . \quad (50)$$

If the automobile is assumed to be driven on a constant-radius circle, that is, $R$ is a constant, it is seen that the required steering angle, $\delta)_{ss}$, will

(1) increase with increasing centrifugal acceleration if $K>0$,

(2) decrease with increasing centrifugal acceleration if $K<0$, and

(3) remain constant if $K = 0$.

Again it is demonstrated that a so-called understeer vehicle has a positive value of $K$ and therefore a positive static margin or positive directional stiffness. A so-called oversteer vehicle has a negative value of $K$ and therefore a negative static margin. Similarly, a neutral-steer vehicle has a value of $K$ equal to zero and therefore has zero static margin.

Equations (48) and (50) are accordingly equivalent and steady-state response tests performed with the test Buick have yielded response data which verify equation (48) as a valid theoretical representation of the steady-state behaviour of the vehicle. Fig. 22 shows experimental steady-state yawing-velocity response data plotted *versus* forward velocity for six separate stability configurations of the test car. On this figure five of the configurations represent a car with varying degrees of understeer or positive static margin. Configuration E was an oversteer vehicle or one with a negative static margin. Measured yawing velocity responses are indicated by the various data points and the solid lines are response curves produced by equation (48) when the values of the constant $K$ shown in Fig. 22 are used. On the basis of this excellent fit between theory and experiment, for assumed values of static margin, it was concluded that equation (48) adequately describes vehicle steady-state behaviour and that a steady-state turn can be described by linear equations of equilibrium, provided lateral accelerations are held below $0{\cdot}3g$.

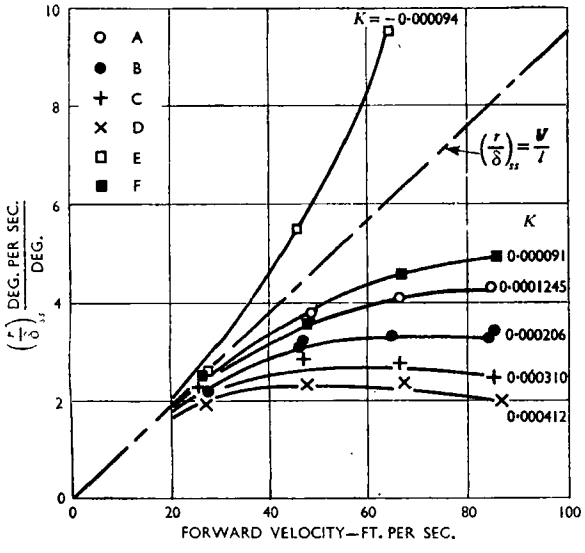


*Fig. 22. Experimental Steady-state Response of Instrumented 1953 Buick*

## Dynamic Stability and Vehicle Modes of Motion

In considering the dynamic behaviour of the automobile, it is pertinent to (1) discuss the stability information which can be extracted from the characteristic equation of the automobile and (2) study the variation in the yawing-velocity response to steering inputs as a function of the static margin and other stability parameters of the vehicle.

The characteristic equation of the automobile as obtained from the derived equations of motion can be expressed as:

$$s^4 + \frac{B}{A}s^3 + \frac{C}{A}s^2 + \frac{E}{A}s + \frac{F}{A} = 0 \quad . \quad . \quad (51)$$

where

$$A = \mu(i_z i_x - i_z m^2 - i^2_{xz})$$

$$B = \mu(m^2 n_r - i_z l_p - n_r i_x - m i_{xz} y_r) - y_\beta i_z i_x - y_\beta i^2_{xz} - i_{xz} m n_\beta$$

$$C = \mu(n_r l_p + n_\beta i_x + m i_z y_\phi - i_z l_\phi - n_\beta m^2 + i_{xz} n_\phi + m i_{xz} y_\beta) + y_\beta i_z l_p + y_\beta n_r i_x - n_\beta y_r i_x$$

$$E = \mu(n_r l_\phi - n_\beta l_p + m n_\phi y_r - m y_\phi n_r) + y_\beta l_\phi i_z - y_\beta n_r l_p + n_\beta y_r l_p + i_{xz} n_\beta y_\phi - i_{xz} y_\beta n_\phi$$

$$F = \mu(m n_\beta y_\phi - m y_\beta n_\phi - n_\beta l_\phi) + n_\beta l_\phi y_r - y_\beta n_r l_\phi$$

In order that the automobile be dynamically stable, that is, the real parts of all roots are negative, a necessary but not sufficient condition is that all of the above coefficients be positive. Numerical studies for the automobile have shown that the stability is a critical function of the constant term, $F/A$, which changes sign under certain conditions. Since the coefficient $A$ is always positive, the dynamic stability is determined by the sign of the coefficient $F$. When $F$ is positive all roots have negative real parts, and when $F$ is negative one unstable mode of motion appears.

Note that this coefficient $F$ as yielded by the expansion of the characteristic determinant, is associated with the steady-state solution of the equations of motion. For example,

$$\frac{r}{\delta}\Big)_{ss} = \frac{1}{\tau}\left[\frac{l_\phi(y_\delta n_\beta - n_\delta y_\beta)}{F}\right] \quad . \quad . \quad (52)$$

Equation (52) is exactly equivalent to equation (47) presented earlier. Thus, the boundary between stability and instability (that is $F = 0$) is identically equivalent to the condition in which the steady-state response becomes infinite. It should be recalled that this situation occurs at that speed at which the damping-in-yaw is sufficiently reduced to the point at which it is effectively cancelled by negative directional stiffness and a positive control input, therefore, produces an infinite response.

The coefficient $F$ can be rewritten to demonstrate that its sign is a function of forward velocity if the static margin

is negative, that is, the vehicle is oversteer. Thus, by ignoring a very small term, $-(n_\beta/y_\beta)y_r$,

$$F = \mu l_\phi y_\beta\left[\left(1-\frac{my_\phi}{l_\phi}\right)\text{S.M.}-\frac{n_r}{\mu}\right] \quad . \quad . \quad (53)$$

or

$$F = \mu l_\phi y_\beta\left[\left(1-\frac{my_\phi}{l_\phi}\right)\text{S.M.}-\frac{lg(\mu n_r)}{V^2}\right] \quad (54)$$

where

$$\mu n_r = -\frac{C}{Mg}\left[\frac{C_2}{C}\left(\frac{2a}{l}-1\right)-\left(\frac{a}{l}\right)^2\right]$$

Equation (54) shows that $F$ can become negative only when the static margin is negative, and that for increasing speeds, an unstable static margin must become less unstable in order to maintain dynamic stability. It should be noted that the quantity within the brackets varies as the square of the forward velocity and that, if it is set equal to zero, it is equivalent to the steady-state criterion for infinite response, that is, $1+KV^2 = 0$.

A solution of the characteristic equation of the automobile generally yields two sets of conjugate complex roots whose real parts are negative. Table 2 shows that these

*Table 2. Representative Solutions of the Characteristic Equation of the 1953 Buick*

| Configuration | Velocity, ft. per sec. | Dimensional roots, 1/sec. | Damped natural frequency, cycles per sec. | Per cent critical damping |
|---|---|---|---|---|
| *Understeer* S.M. = 0·0692 | 25·4 | −1·673 ±6·09i<br>−10·39<br>−16·89 | 0·97 | 0·265 |
| | 46·3 | −2·04 ±6·39i<br>−7·00 ±2·505i | 1·018<br>0·399 | 0·3045<br>0·941 |
| | 83·8 | −2·40 ±7·02i<br>−3·22 ±3·20i | 1·119<br>0·51 | 0·324<br>0·71 |
| | 146·7 | −1·796 ±7·53i<br>−1·671 ±2·78i | 1·199<br>0·443 | 0·232<br>0·516 |
| *Oversteer* S.M. = − 0·0543 | 44·5 | −3·165 ±8·10i<br>−2·515<br>−9·09 | 1·29 | 0·364 |
| | 88 | −2·62 ±9·25i<br>−0·1795<br>−5·05 | 1·473 | 0·273 |
| | 146·7 | −2·185 ±9·59i<br>+0·755<br>−3·805 | 1·527 | 0·2165 |

two convergent or stable periodic modes of motion have damped natural frequencies in the vicinity of 1 cycle and ½ cycle per sec. Numerical studies have shown that the lower frequency mode involves yawing and side-slipping to a significantly greater degree than the higher frequency mode, which appears to consist mainly of rolling motion. Although the close proximity in frequency makes it very difficult to factor accurately the quartic into two quadratics, one for each mode, an approximate factorization yields the following result:

$$s^4+\frac{B}{A}s^3+\frac{C}{A}s^2+\frac{E}{A}s+\frac{F}{A} \cong (s^2+bs+k)(s^2+b's+k') \quad (55)$$

where

$$b = -\left(\frac{y_\beta}{\mu}+\frac{n_r}{i_z}\right)$$

$$k = \frac{y_\beta n_r}{\mu i_z}+\frac{n_\beta}{i_z}+\frac{n_\phi m y_\beta}{i_z l_\phi}$$

$$b' = -\frac{l_p}{i_x-m^2}$$

$$k' = -\frac{l_\phi}{i_x-m^2}$$

Examination of these two second-order modes, represented by the two quadratic factors of the original fourth-order system, reveals that the first quadratic is closely related to the characteristic equation yielded by a non-rolling automobile, whereas the coefficients of the second quadratic factor consist only of vehicle roll parameters, $l_\phi$, $l_p$, $i_x$, and $m$. This result does indeed indicate that the first mode is a yawing and side-slipping mode, while the second is primarily a rolling mode of motion.

If attention is directed to the roots of the yawing and side-slipping mode, it is found numerically that these roots simplify to the following form:

$$\lambda_1, \lambda_2 = \frac{1}{\tau}\left[\tfrac{1}{2}\left(\frac{y_\beta}{\mu}+\frac{n_r}{i_z}\right)\pm\sqrt{\frac{n_\beta+\dfrac{n_\phi m y_\beta}{l_\phi}}{i_z}}\right] \quad (56)$$

On reference to the definition of static margin for a rolling vehicle, it is seen that equation (56) may be rewritten, with the assumption that $my_\phi$ is negligible in comparison with $l_\phi$, to result in the following expression for the roots $\lambda_1$, and $\lambda_2$.

$$\lambda_1, \lambda_2 = \frac{1}{\tau}\left[\tfrac{1}{2}\left(\frac{y_\beta}{\mu}+\frac{n_r}{i_z}\right)\pm\sqrt{\frac{y_\beta(\text{S.M.})}{i_z}}\right]. \quad (57)$$

Equation (57) shows that the expression S.M. = 0 is the boundary condition between an oscillatory mode and two distinct aperiodic modes of motion. Generally speaking, when the vehicle is understeer (static margin is positive), the complete characteristic quartic has two conjugate complex roots. When the vehicle is oversteer, there is one conjugate complex root and two real negative roots. As speed of the oversteer vehicle is increased, however, one negative real root approaches zero and eventually becomes positive at the instant the coefficient, $F$, of the characteristic equation becomes negative (Table 2). Note that the damping of the directional mode is produced by the damping-in-sideslip, $y_\beta$, and the damping-in-yaw, $n_r$. Equation (57) shows that behaviour of the directional mode will vary widely as the static margin goes from positive to negative and as the damping decreases with increasing forward velocity of the vehicle.

Transforming the roots represented by equation (57) to the form in which they are functions of the basic dimensional properties of a vehicle proves to be extremely informative and enlightening. If the excellent approximation is made that $n_r = y_\beta/4\mu$, equation (57) may be written as

$$\lambda_1 \lambda_2 = \tfrac{1}{2}\frac{C}{MV}\left[1+\frac{1}{4\left(\frac{k_z}{l}\right)^2}\right] \pm \sqrt{\frac{\frac{C}{Ml}(\text{S.M.})}{(k_z/l)^2}} \quad (58)$$

Thus, the damping of the directional mode

(1) increases with increasing total cornering stiffness of the vehicle,
(2) increases with decreasing mass of the vehicle,
(3) decreases with increasing speed of the vehicle, and
(4) increases with decreasing ratio of radius of gyration in yaw to vehicle wheelbase.

The frequency, on the other hand, is defined only for positive values of static margin and

(1) increases with increasing total cornering stiffness,
(2) increases with decreasing vehicle mass,
(3) increases with increasing static margin, and
(4) increases with decreasing ratio of radius of gyration in yaw to vehicle wheelbase.

## The Transient Response to Steering Inputs

Examination of the characteristic equation of the automobile has indicated the frequency and damping of the modes of motion of the automobile and produced a simple criterion for dynamic stability. Additional information on the nature of the response of the vehicle to steering control is obtained by solving the equations of motion to yield the response to front-wheel displacement as influenced by static margin, forward velocity, yawing moment of inertia, roll steer, roll stiffness, etc. This type of study is conveniently performed on an analogue computer or, lacking a computer, is best handled with the aid of the operational calculus.

As an example, Fig. 23 has been prepared to show the effects of static margin on the yawing-velocity response of the Buick to a step input of front-wheel angle. Response time histories are shown for an 'under-', 'neutral-', and 'oversteer' configuration at 60 m.p.h. Note that at this speed the oversteer vehicle is just on the verge of becoming unstable. (This means that a few more m.p.h. of forward velocity would cause one root of the characteristic equation to become zero, in which case the yawing-velocity response would increase linearly with time after the stable modes damped out. Additional speed would then cause the response curve to become concave upward.) These three time histories show that the directional stiffness, as calculated in terms of the static margin, has an appreciable effect on both the transient response and the steady-state response or 'static sensivity'.

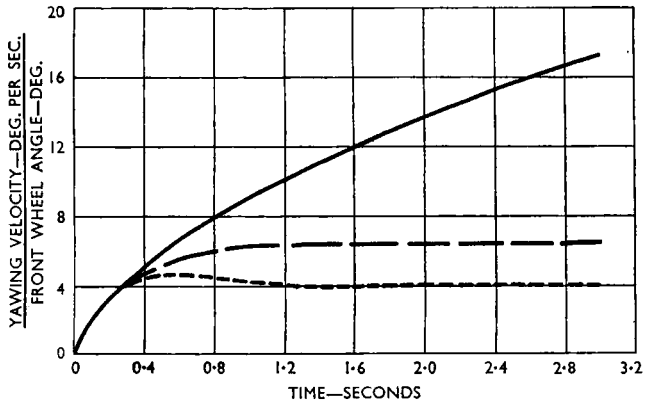


*Fig. 23. Influence of Static Margin on the Yawing-velocity Transient Response to a Step Input of Front-wheel Angle*

$V = 60$ m.p.h.
———— Static margin = −0·05.
— — — Static margin = 0.
– – – – – Static margin = +0·068.

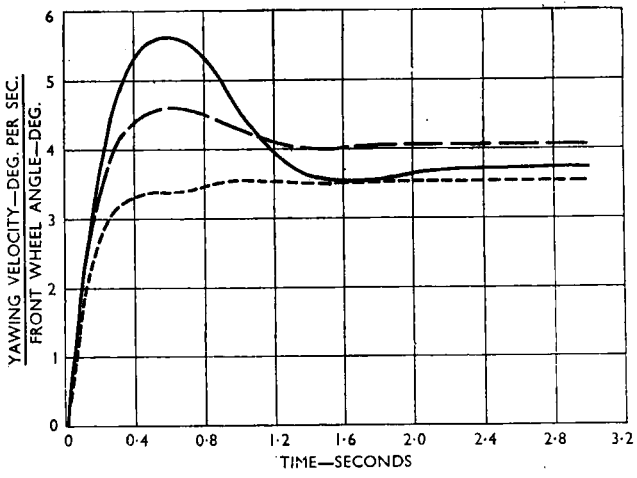


*Fig. 24. Influence of Forward Velocity on the Yawing-velocity Transient Response of an Understeer Vehicle*

Static margin = +0·068.
———— $V = 90$ m.p.h.
— — — $V = 60$ m.p.h.
– – – – – $V = 30$ m.p.h.

Fig. 24 shows the influence of forward velocity on the response of an understeer Buick. The decrease in directional damping with increasing speed is primarily responsible for the observed change in transient behaviour. It should be pointed out that the overshoot characteristic will be still larger at speeds higher than that shown and that the over-all behaviour of the understeer car is in sharp contrast to that presented in Fig. 25 for an oversteer Buick. For the oversteer case, no overshoot characteristic is encountered with increased speed. Instead the response becomes slower, while the static sensitivity increases abruptly with increase in speed. It is seen that the test car with S.M. = −0·05 is dynamically unstable at 90 m.p.h.

The influence of static margin on the yawing-velocity response can also be observed on the frequency-response plot. For example, Fig. 26 gives the yawing-velocity response divided by the steady-state response, for both the standard-instrumented and oversteer configurations of the Buick at 60 m.p.h. (These response curves are called 'normalized' because the effects of static sensitivity have been removed in order to show the difference in dynamic behaviour.) The extremely rapid fall off in response amplitude with increasing frequency shows that, dynamically speaking, the response of the oversteer vehicle is significantly slower than that of the understeer vehicle. This result is in agreement with the time histories shown in Fig. 23, where it is seen that the oversteer response will take a very long time to reach the steady state.

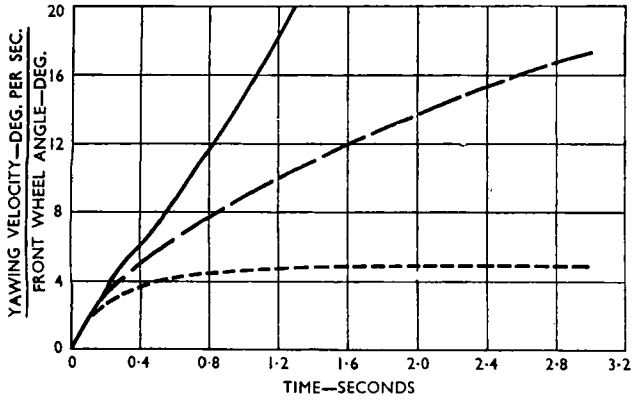


*Fig. 25. Influence of Forward Velocity on the Yawing-velocity Transient Response of an Oversteer Vehicle*

Static margin = −0·05.

——— $V$ = 90 m.p.h.
— — — $V$ = 60 m.p.h.
– – – – – $V$ = 30 m.p.h.

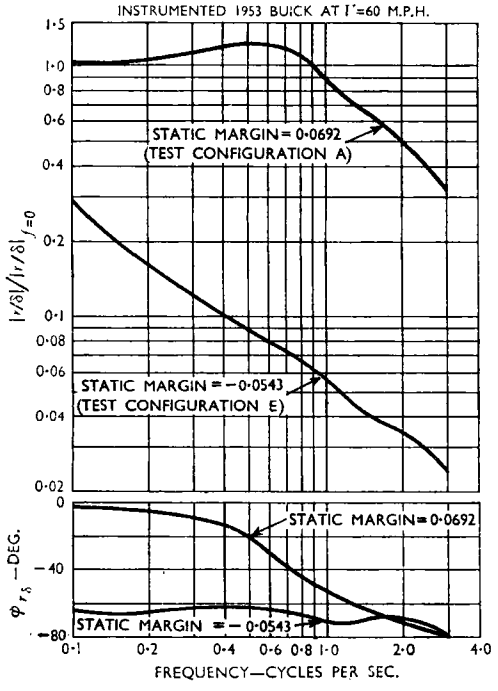


*Fig. 26. Influence of Static Margin on the Yawing-velocity Frequency Response*

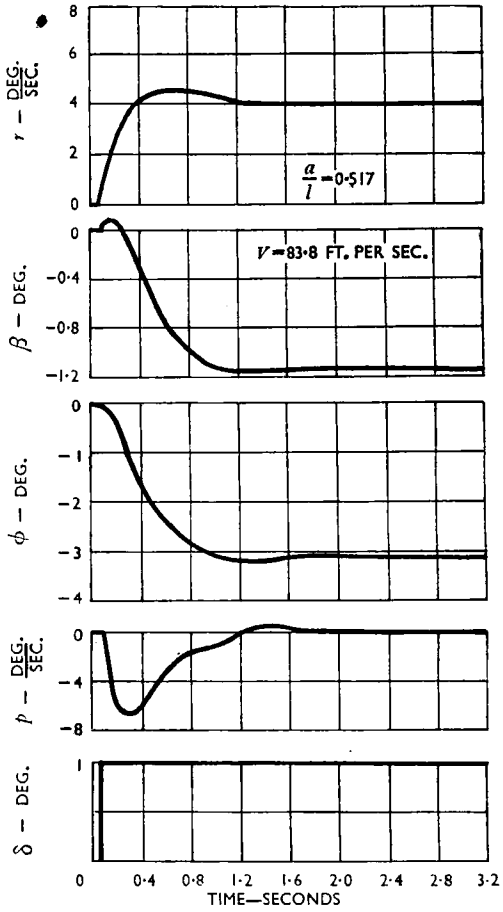


*Fig. 27. Lateral Response of Buick to Step Input of Front-wheel Angle*

Figs. 23, 24, 25, and 26 summarize the manner in which static margin and forward velocity affect the transient response of an automobile to steering control. In a similar fashion, studies may be made of the effects of yawing moment of inertia, roll stiffness, roll steer, height of c.g. of rolling mass above roll axis, etc., on the lateral-response characteristics of a pneumatic-tyred vehicle. Such studies are, of course, expedited with the use of analogue computers, and Fig. 27 is presented herein as a typical example of a solution yielded by commercially available electronic analogue simulation equipment.

## CONCLUSIONS

In this paper an attempt has been made to summarize the investigations, both theoretical and experimental, made by C.A.L. in the field of automotive directional stability and

control. In so doing, the following three major items were treated:

(1) Development of a mathematical model of the automobile.

The restrictions placed on the types of force encountered by the automobile and the types of input to this dynamic system were set forth, together with all additional assumptions and approximations. After the inertia-reaction terms were presented, the external forces and moments were evaluated, by means of a stability-derivative notation, the usefulness of which had been previously demonstrated in studies of aircraft stability and control. The resulting equations of motion were then non-dimensionalized in order to increase their utility in general studies of vehicle dynamic behaviour.

(2) Experimental substantiation of the derived equations of motion.

Some of the techniques used to determine the basic properties of the test vehicle, such as its inertia, chassis and tyre characteristics, were indicated briefly. This discussion was followed by a description of (*a*) the instrumentation of the test vehicle, (*b*) testing procedures, and (*c*) data-reduction methods. Sample dynamic-response data were presented in frequency-response form and test results were compared with theoretical predictions.

(3) Discussion of the manner in which the automobile responds to steering control.

The directional behaviour of the automobile was described by examining both the steady-state and transient response to front-wheel steering inputs. In this manner the influence of static margin on the steady-state yawing-velocity response was investigated, with vehicle directional stability (static margin) demonstrated to be equivalent to the under/oversteer concepts developed by Olley.[45] The transient-response characteristics were discussed by (*a*) examining the modes of motion yielded by a solution of the vehicle's characteristic equation and (*b*) observing the variation in yawing-velocity response as a function of vehicle static margin and forward velocity.

As a result of the research effort summarized above, it was concluded that:

(1) The derived equations of motion and their subsequent verification by full-scale response tests have to date defined the lateral dynamic behaviour of the fixed-control automobile on a level road.

(2) This work will eventually lead to a full understanding of the rigid-body mechanics of the automobile, provided that additional research and test programmes are run in the fields of vehicle aerodynamics and tyre mechanics.

(3) The assumption of linearity, together with the use of stability derivative notation, has greatly simplified the treatment and understanding of automotive directional stability and control.

(4) The terms understeer and oversteer, though acceptable for the purposes of describing directional stability, are lacking in precise meaning when discussing the effects of directional stability (stiffness) on:

(*a*) dynamic stability,
(*b*) the transient response, and
(*c*) the steady-state response (static sensitivity).

(5) The effects of tyre dynamics (that is, lags between tyre slip angle and tyre force) on the lateral response of the automobile are very small at oscillation frequencies below 3 cycles per sec.

## ACKNOWLEDGEMENTS

The author acknowledges, with many thanks, the assistance and co-operation of his colleagues in the Flight Research and Vehicle Dynamics Departments of C.A.L. and the invaluable aid of personnel of the General Motors Corporation and the United States Rubber Company. In particular, acknowledgement is made to Mr. J. Bidwell, for permission to publish this information, and to Mr. A. Pulley, who was responsible for instrumenting the test vehicle, and who assisted the author throughout the test programme.

## APPENDIX IV

### INSTRUMENTATION OF THE TEST VEHICLE

The design, fabrication, installation, and calibration of a dynamic recording system constituted the instrumentation phase of the research described in this paper. The solution of this task was expedited by the experience accumulated at C.A.L. in performing similar projects with aircraft.

Fig. 28 is a block diagram of the installation used to measure the rigid-body motions of the test Buick. The diagram shows that the transducer recording system was a direct-current system, with the exception of the rate gyros which had their own power supply and demodulator unit. Two 12-V. batteries were connected in series to provide power for the recording oscillograph, the rate-gyro power supply, and driving the gyro wheel of the attitude gyro. The direct-current bridge supply, for all instruments except the rate gyros, was obtained from 6-V. dry cells.

Most of the instrumentation was installed in the trunk. In Fig. 29, Plate 1, are visible the two batteries used for the basic power supply, the power supply and demodulator unit for the two Doelcam rate gyros, the galvanometer filter and terminal box, and the Consolidated 18-channel recording oscillograph. Behind the meter panel, from left to right, are the bridge-voltage supply batteries, the Doelcam rate gyros, and the Minneapolis-Honeywell attitude gyro. The lateral accelerometer was mounted on the chassis frame with three mounting locations provided for locating the accelerometer in the lateral $y$–$z$ plane, which contains the c.g. of the car. Angular rotation of the front wheels was measured by an angular potentiometer mounted on the front-wheel backing plate, and driven by an extension of the kingpin. Steering-wheel position was measured by an angular accelerometer mounted on the steering column.

In the early stages of this research, it was assumed that information would be recorded in the frequency range of 0 to 10 cycles per sec. This assumption was quickly modified after the first 'shake-down' runs, which indicated that both engine vibrations and wheel hop were being picked up by the measuring transducers. This result indicated that subsequent data reduction would be very uncertain. On reconsidering the necessary frequency range required to define the automobile's rigid-body dynamics, the research group decided to record information from 0 to 3 cycles

per sec, and to attempt to attenuate all frequencies above this range as much as possible. Filters were designed to do this, particularly for the rolling-velocity and lateral-acceleration channels, which were especially sensitive to engine and road disturbances. Extremely effective results were obtained with the tuned galvanometer circuits to be discussed in a subsequent paper by Muzzey and Close.

## APPENDIX V

### REFERENCES

All references (identified by superscript numbers) in this paper will be found in the master reference list given in Appendix III of Paper I.

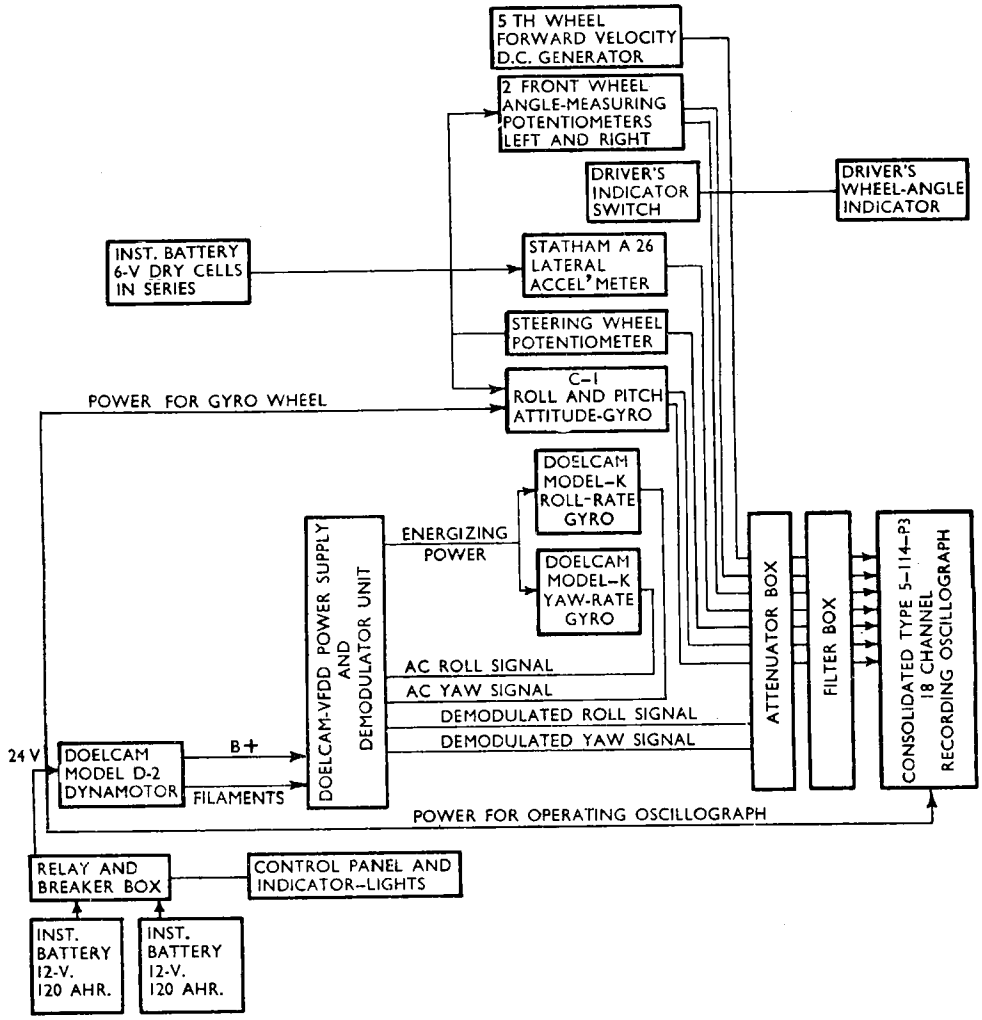


*Fig. 28. Block Diagram of Instrumentation in Test Car*